CONFIDENTIAL

COPY NO.
RM No. E7D28

NACA

RESEARCH MEMORANDUM

SOME METHODS OF ANALYZING THE EFFECT OF BASIC DESIGN VARIABLES ON AXIAL-FLOW-COMPRESSOR PERFORMANCE

By John T. Sinnette, Jr.

Flight Propulsion Research Laboratory
Cleveland, Ohio

CLASSIFIED DOCUMENT

This document contains classified information affecting the National Defense of the United States within the meaning of the Espionage Act, USC 50:31 and 32. Its transmission or the revelation of its contents in any manner to an unauthorized person is prohibited by law. Information so classified may be imparted only to persons in the military and naval services of the United States, appropriate civilian officers and employees of the Federal Government who have a legitimate interest therein, and to United States citizens of known loyalty and discretion who of necessity must be informed thereof.

NATIONAL ADVISORY COMMITTEE FOR AERONAUTICS

WASHINGTON

November 26, 1947

NATIONAL ADVISORY COMMITTEE FOR AERONAUTICS

RESEARCH MEMORANDUM

SOME METHODS OF ANALYZING THE EFFECT OF BASIC DESIGN VARIABLES ON AXIAL-FLOW-COMPRESSOR PERFORMANCE

By John T. Sinnette, Jr.

SUMMARY

A blade-element theory for axial-flow compressors has been developed and applied to the analysis of the effects of basic design variables on compressor performance. Charts, which are useful for a wide variety of design calculations, are presented. The relation between several efficiencies useful in compressor design are derived and discussed, and the blade-element efficiency is shown to be given by the same expression as that for the profile efficiency of a propeller. The possible gains in useful operating range obtainable by the use of adjustable stator blades are discussed and a rapid method of calculating blade resettings using charts is shown by an example.

The relative Mach number is shown to be a dominant factor in determining the pressure ratio. If suitable efficiencies can be maintained, very high pressure ratios per stage are possible with supersonic designs. But even for subsonic compressor designs, considerable increase in pressure ratio over that for conventional designs can be obtained by producing a velocity distribution that gives relative inlet Mach numbers close to the limiting Mach number on all blade elements. With a given inlet Mach number, the pressure ratio obtainable across a blade row increases and the specific mass flow decreases as the ratio of mean whirl velocity to axial velocity increases for the high-efficiency range of this velocity ratio.

For subsonic compressor designs with a definite Mach number limitation, the velocity distribution in the inlet stage is particularly important because the inlet stage limits both the mass flow and the rotor speed of the compressor and thereby limits the pressure ratio of the later stages as well as the inlet stage. By the use of entrance guide vanes designed to produce a variable axial velocity at the entrance to the first rotor, a substantial increase in stage pressure ratio and a slight increase in specific

mass flow over designs based on free vortex with the same turning and Mach number limitations are shown to be possible. In the succeeding stages, the maximum pressure ratio per stage is obtained by increasing the hub diameter to obtain the maximum axial velocity compatible with the Mach-number limitation.

INTRODUCTION

The limited amount of research information available for the design of turbojet and turbine-propeller engines has emphasized the need for fundamental research on the compressor as one of the principal components of these power plants. The compressor characteristics that must be considered in the research program are efficiency, size and weight, and operating range, or flexibility.

Efficiency has a pronounced effect on the specific fuel consumption of the engine and is therefore especially important for long-range nonstop flights where the fuel weight may amount to several times the useful pay load. Although the efficiency of modern axial-flow compressors is high compared with other types of compressor, substantial gains in engine performance can be derived from further improvement in efficiency.

The importance of size and weight per unit power output of the engine increases rapidly as the flight speed is increased because of the rapid increase in the power required. For some of the high-speed aircraft being developed, the consideration of the size and the weight of the power plant becomes of the utmost importance. This analysis is primarily concerned with the compressor size as given by its diameter and length and therefore considers the weight only as affected by these variables. The length of a compressor for a given pressure ratio is determined by the pressure ratio per stage and the axial length of a stage; the diameter for a given air flow is determined by the air flow per unit cross-sectional area and by the percentage of the total frontal area utilized. Because of the relatively low pressure ratio per stage, the length of an axial-flow compressor is usually greater than that of a centrifugal compressor, but the over-all diameter is smaller because of the utilization of a larger percentage of the over-all frontal area for air intake. Special effort should therefore be given to reducing the length of an axial-flow compressor with a given over-all pressure ratio by increasing the pressure ratio per stage. Reduction in the diameter for a given air flow by increasing the flow per unit inlet area is also advantageous, particularly for supersonic aircraft, where frontal area is extremely important.

For operation at other than design conditions, the compressor range, or flexibility, becomes important. At engine speeds below the design value, the compressor efficiency may be low because of a drop in peak efficiency or because of improper matching of the compressor with the turbine. Consequently, the power required to start the engine may be high and the acceleration to design speed, slow. Because of improper matching, compressor surging may be encountered at intermediate speeds, particularly during rapid acceleration. The engine starting and accelerating characteristics with axial-flow compressors are generally poorer than with centrifugal compressors mainly because the efficiency is highest at relatively high compressor speeds and drops appreciably as the speed is reduced. The use of high pressure ratios to improve the cycle efficiency accentuates the problems associated with starting and accelerating to design speed and emphasizes the need for the improvement of the range of the compressor.

The effect of basic design variables on efficiency, pressure ratio, and mass flow in axial-flow compressors is analyzed in terms of blade-element theory, which is an extension of the theories developed in references 1 and 2. The blade-element analysis neglects the effects of variations in velocity, pressure, and density in the tangential direction at any given axial station. On this basis, the flow across a blade row is treated as a steady, one-dimensional, adiabatic, compressible flow, and the velocity ratio, pressure ratio, density ratio, and velocity-of-sound ratio are expressed in terms of the flow-area ratio and the polytropic compression efficiency. Charts are presented for the rapid determination of these ratios for polytropic compression efficiencies from 0.7 to 1.0. As no restriction is placed upon the variation in axial velocity across a blade row, the method and the charts are applicable to a wide variety of compressor-design problems.

In order to investigate the effect of the ratio of mean whirl velocity to axial velocity on the efficiency and the pressure ratio, a blade-element theory of efficiency based upon incompressible flow and constant axial velocity is developed. The pressure ratio, for constant axial velocity and compressible flow, is then expressed in terms of the blade-element drag-lift ratio and the ratio of mean whirl velocity to axial velocity, by using the general theory for pressure ratio and assuming that the polytropic efficiency is equal to the efficiency obtained from the incompressible-flow theory. The effect of the ratio of the mean whirl velocity to axial velocity on the specific mass flow

is also derived in terms of compressible-flow theory. A simplification of the method of calculating blade resettings for different operating conditions based on the use of charts developed in this report is presented.

SYMBOLS

The symbols used in this report are defined in alphabetical order. The quantities represented by the symbols f, M, V, w_m, and β depend upon the reference frame. When only a single row of blades is being considered, that row of blades is taken as the reference frame. In consideration of a complete stage or any other cases where the reference frame is not clear, it is indicated by the subscript R or S for rotor or stator, respectively.

A	cross-sectional area, square feet
a	velocity of sound, feet per second
C_D	drag coefficient
C_L	lift coefficient
c	blade chord, feet
c_p	specific heat at constant pressure, Btu per pound ^oF
c_v	specific heat at constant volume, Btu per pound ^oF
D	blade-profile drag, pounds per foot
F	resultant force per unit blade length, pounds per foot
f	flow area $(A \cos \beta)$, square feet
g	standard acceleration of gravity, 32.174 feet per second per second
h	static enthalpy per unit mass, foot-pounds per slug
J	mechanical equivalent of heat, 778 foot-pounds per Btu
K	constant in turning-angle relation
L	blade-profile lift, pounds per foot

l	blade height, feet
M	local Mach number (V/a)
m	polytropic exponent for compression
P	total pressure, pounds per square foot absolute
p	static pressure, pounds per square foot absolute
R	gas constant, foot-pound per pound $^{\circ}R$
r	radius to blade element, feet
S	blade spacing at radius r, feet
T	total temperature, $^{\circ}R$
t	static temperature, $^{\circ}R$
U	velocity of blade (ωr) at radius r, feet per second
V	air velocity with respect to reference frame, feet per second
W	mass flow rate, pounds per second
$W\sqrt{\theta}/\delta$	mass flow rate corrected to standard sea-level pressure and temperature, pounds per second
$W\sqrt{\theta}/(\delta A)$	specific mass flow, pounds per second per square foot
w_m	ratio of mean whirl velocity to axial velocity (fig. 1)
$-\Delta w$	ratio of decrease in whirl velocity to axial velocity (fig. 1)
$\alpha_{a,o}$	angle of attack of isolated airfoil for zero lift, degrees
β	angle between compressor axis and air velocity, or flow angle (fig. 1), degrees
γ	ratio of specific heats (c_p/c_v)
δ	ratio of inlet total pressure to standard sea-level pressure (2116.2 lb/sq ft)

ϵ	gliding angle $(\tan^{-1} D/L)$
η_{ad}	adiabatic efficiency of compression based on static pressure and temperature
η_p	polytropic efficiency of compression based on static pressure and temperature
η_{st}	compression efficiency based on static pressure
θ	ratio of inlet total temperature to standard sea-level temperature (518.6° R)
ρ	density, slugs per cubic foot
σ	blade-element solidity (c/S)
ψ	angle between blade chord and compressor axis, degrees
ω	absolute angular velocity of blade, radians per second

Subscripts:

0	standard sea-level conditions
1	inlet to blade row or stage
2	outlet of blade row
3	outlet of stage
a	axial
an	annulus
h	hub
i	incompressible
id	ideal
m	referred to vector-mean velocity
R	rotor
S	stator
s	secondary

st	static
T	total
t	rotor-blade tip
w	whirl
θ	tangential

BLADE-ELEMENT THEORY

The blade-element theory is divided into four parts: (1) gives the general compressible-flow theory in terms of polytropic compression efficiency; (2) develops the theory of blade-element efficiency in terms of incompressible flow and constant axial velocity; (3) combines the results of the first two parts to obtain the pressure ratio as a function of the drag-lift ratio and the ratio of mean whirl velocity to axial velocity for constant axial velocity; (4) considers the specific mass flow in terms of compressible-flow theory.

Compressible-Flow Theory

One-dimensional analysis. - Because of the extreme complexity of the actual flow through compressor blades, various approximate methods of analysis are necessary. Analysis based upon one-dimensional flow, given in various forms and involving various approximations, has proved useful in the analysis of the flow through compressors and turbines and as a basis for design. (See, for example, references 3 to 5.) With an infinite number of blades, a perfect compressible fluid theoretically flows along surfaces of revolution, which constitute flow surfaces, and the velocity, the pressure, and the density are independent of the circumferential position. Because these flow variables may be expressed as a function of a single coordinate of position for the flow between two infinitely close stream surfaces, this flow may be considered as "one-dimensional" flow. The actual determination of the stream surfaces, of course, constitutes a separate problem.

The flow of a real fluid through a finite number of blades, however, is dependent on the circumferential position because of the effects of finite blade circulation, viscosity, and turbulence,

and the flow will not follow exactly along surfaces of revolution. A one-dimensional approximation to the actual flow may be obtained, however, by using values of velocity, pressure, and density averaged in the circumferential direction and by using, for mean stream surfaces, surfaces of revolution through which the average net flow at any axial position is zero. Because the total flow of energy across a surface through which the fluid is flowing is greater than that based upon mean flow (reference 6), this simple one-dimensional analysis gives an inaccurate representation of the energy flow at stations where there are large circumferential variations in velocity or a high degree of turbulence. A more accurate analysis could be obtained by using suitable coefficients to correct for effects of nonuniform velocity and turbulence. Because the present analysis is applied only to stations between blade rows where the circumferential variations are normally small, and because the corrections for turbulence are very complex (reference 6), these refinements are omitted.

Consider the flow across a row of rotor blades between two infinitely close surfaces of revolution corresponding to mean stream surfaces and take a reference frame that is fixed with respect to the blades so that the flow is essentially steady. If the energy transfer across the boundary surfaces of revolution is neglected, the energy equation for the flow across the blade row (fig. 1(a)) can be written

$$\frac{V_1^2}{2} - \frac{V_2^2}{2} + \frac{\omega^2 r_2^2}{2} - \frac{\omega^2 r_1^2}{2} = gJc_p t_1 \left(\frac{t_2}{t_1} - 1 \right) \tag{1}$$

The terms involving the angular velocity of the reference frame ω represent the change in potential energy of the centrifugal-force field that results from the rotating frame of reference. The equation can, of course, be obtained by first considering the energy equation for a nonrotating reference frame and then transforming the results to the rotating reference frame. The expression of t_1 in terms of velocity of sound a_1 gives, after slight rearrangement,

$$\frac{t_2}{t_1} = 1 + \frac{\gamma - 1}{2} M_1^2 \left[1 - \left(\frac{V_2}{V_1} \right)^2 + \left(\frac{\omega r_2}{V_1} \right)^2 - \left(\frac{\omega r_1}{V_1} \right)^2 \right] \tag{2}$$

For the flow through the stator blades the reference frame is stationary and ω is equal to 0. The temperature ratio, for a given inlet Mach number M_1 and velocity ratios V_2/V_1, $\omega r_2/V_1$,

and $\omega r_1/V_1$, does not depend upon losses, but the pressure ratio p_2/p_1 and density ratio ρ_2/ρ_1 do. The pressure ratio, density ratio, and velocity-of-sound ratio a_2/a_1 can be expressed in terms of the temperature ratio by use of the polytropic relation

$$\frac{p_2}{p_1} = \left(\frac{\rho_2}{\rho_1}\right)^m$$

the equation of state for a perfect gas

$$p/\rho = gRt$$

and the equation for the velocity of sound

$$a = \sqrt{\gamma g R t}$$

The resulting relations can be concisely written as

$$\frac{p_2}{p_1} = \left(\frac{\rho_2}{\rho_1}\right)^m = \left(\frac{t_2}{t_1}\right)^{\frac{m}{m-1}} = \left(\frac{a_2}{a_1}\right)^{\frac{2m}{m-1}} \tag{3}$$

The value of m depends upon the losses and can be expressed in terms of the polytropic compression efficiency discussed in the following section.

The continuity equation, applied to the flow between the two infinitely close stream surfaces and expressed in terms of the flow area f measured normal to the relative velocity, is

$$\frac{f_1}{f_2} = \frac{2\pi r_1 \, dr_1 \cos \beta_1}{2\pi r_2 \, dr_2 \cos \beta_2} = \frac{\rho_2 V_2}{\rho_1 V_1} \tag{4}$$

The density can be eliminated from equation (4) by means of equations (2) and (3) to obtain the flow-area ratio as an explicit function of the velocity ratios, the inlet Mach number, and the polytropic exponent:

$$\frac{f_1}{f_2} = \frac{V_2}{V_1}\left\{1 + \frac{\gamma-1}{2} M_1^2 \left[1 - \left(\frac{V_2}{V_1}\right)^2 + \left(\frac{\omega r_2}{V_1}\right)^2 - \left(\frac{\omega r_1}{V_1}\right)^2\right]\right\}^{\frac{1}{m-1}} \tag{5}$$

For axial-flow compressors, radial flow can usually be neglected; consequently r_1 equals r_2 and equation (5) becomes

$$\frac{f_1}{f_2} = \frac{V_2}{V_1}\left\{1 + \frac{\gamma-1}{2} M_1^2 \left[1 - \left(\frac{V_2}{V_1}\right)^2\right]\right\}^{\frac{1}{m-1}} \tag{6}$$

which does not contain ω and hence has the same form for rotating and stationary blades. It should be noted that the velocities are with respect to the given blade row as reference frame.

Graphical representation in terms of polytropic efficiency. - A graphical representation of equation (6) is useful for the rapid determination of any one of the variables in terms of the others. As it is usually more convenient to think in terms of compression efficiency than in terms of polytropic exponent, the graphical representation of equation (6) is given in terms of the polytropic compression efficiency. This efficiency differs in two respects from the usual compressor efficiency. Compressor efficiency is usually defined as the ratio of the ideal work of compression from the initial to the final total pressure to the actual work done by the rotor blades. This efficiency is satisfactory for over-all performance representation but gives no information on the efficiency with which static pressure is increased and is meaningless when applied to stationary elements of the compressor (stator blades and exit diffuser). As a measure of efficiency of the separate steps in the compression process, an efficiency based upon static pressure is therefore required. The change in kinetic energy of the fluid as well as the work input by the rotor blades is available for conversion to static pressure. For rotating reference frames the change in potential energy of the centrifugal-force field, which occurs when the radius changes, is also available for increasing the static pressure. If there is no heat transfer, the energy available for conversion into pressure is given by the change in static enthalpy Δh, whereas the ideal energy required for the given pressure change is

$$\int_{p_1}^{p_2} \frac{dp}{\rho_{id}(p)}$$

where $\rho_{id}(p)$ is the density as a function of pressure for the ideal compression process. The general definition of efficiency based on the conversion of mechanical energy into static pressure is therefore

$$\eta_{st} = \frac{\int_{p_1}^{p_2} \frac{dp}{\rho_{id}(p)}}{\Delta h} \tag{7}$$

and differs from the corresponding efficiency based on total pressure only in the replacement of enthalpies and pressures based on total (stagnation) conditions by those based upon static conditions. Unlike the efficiency based upon total conditions, the efficiency based upon static conditions is independent of the reference frame and can be applied equally well to stationary and rotating components of the compressor. For these reasons, an efficiency based on static conditions is used for the graphical representation.

The efficiency is incompletely specified, however, until the ideal process of compression is given. Herein lies the other difference between the efficiency used in this analysis and the conventional adiabatic compressor efficiency. For compression without heat transfer, the relation between adiabatic and polytropic efficiency is shown in appendix A to be given by

$$\eta_{ad} = \frac{\left(\frac{p_2}{p_1}\right)^{\frac{\gamma-1}{\gamma}} - 1}{\left(\frac{p_2}{p_1}\right)^{\frac{\gamma-1}{\gamma\eta_p}} - 1} \tag{8}$$

for efficiencies and pressure ratio based on either total or static conditions. When the pressure ratio is plotted on a logarithmic scale (fig. 2), a practically straight-line relation is obtained with the two efficiencies equal at a pressure ratio of 1. For the pressure ratios obtained across a row of blades, at least for subsonic designs (generally less than 1.2), the difference between adiabatic and polytropic efficiencies is negligible (fig. 2). It is shown in appendix A that the polytropic exponent for compression is given in terms of the polytropic efficiency by the relation

$$m = \frac{\eta_p}{\eta_p - \frac{\gamma-1}{\gamma}} \qquad (9)$$

The discussion on efficiency may be summarized: The difference between the adiabatic and polytropic efficiencies is usually negligible for the pressure ratios obtainable across a blade row or a stage but becomes important when the over-all efficiency of a compressor is considered. The chart relating the two efficiencies (fig. 2) is useful in estimating the over-all adiabatic efficiency of a compressor for adiabatic compression in terms of an average stage efficiency represented by the polytropic efficiency. Efficiencies based on static pressure and temperature changes are required in considering the compression across individual blade rows and the same basis for efficiency can be used for over-all compressor-performance representation. If the conventional adiabatic efficiency for the over-all performance in terms of total pressures and temperatures is desired, a small correction may be applied to the adiabatic efficiency based on static states to take account of the change in Mach number across the compressor.

By means of equations (6) and (9), the flow-area ratio f_1/f_2 can be expressed as an explicit function of the inlet Mach number, the velocity ratio, and the polytropic efficiency. The relation between these variables is shown in figure 3. By use of equations (2), (3), and (9) (with $r_1 = r_2$), the velocity-of-sound ratio a_2/a_1, temperature ratio t_2/t_1, density ratio ρ_2/ρ_1, and pressure ratio p_2/p_1 may also be given in terms of the same variables. For the applications considered, however, it is more convenient to replace the velocity ratio by the flow-area ratio as one of the independent variables by means of equation (6). The graphical representation of these ratios with the inlet Mach number, flow-area ratio, and polytropic efficiency as independent variables is shown in figure 4. Figures 3 and 4 show that the polytropic efficiency has a rather large effect on the flow relations especially at high Mach numbers. Appreciable error in the velocity ratios for a given type of blading may therefore result if the calculations are based upon isentropic flow.

A rigorous application of the charts to general blade-element analysis requires additional relations based on considerations of radial equilibrium and will not be further developed here. The charts, however, may be used for rapid approximate design calculations and for the calculation of blade resettings for different

operating conditions by considering only mean conditions for the entire annular passage. An example of this type of application is given in appendix B.

Blade-Element Efficiency

The exact analysis of the efficiency of an axial-flow compressor is extremely complex and must be based upon a detailed knowledge of the flow processes involved. An approximate analysis can, however, be made by treating the flow and the corresponding losses near the ends of the blades separately from those for the central portion of the annular passage. The present blade-element analysis is applicable to the main portion of the flow. The losses near the ends of the blades will be discussed under the section entitled "Application of Blade-Element Theory to Compressor Design." The following analysis of the blade-element efficiency is based upon the assumptions of incompressible flow, constant axial velocity (see fig. 1(b)), and no radial flow. The usual magnitudes of radial flow, variations in axial velocity, and compressibility effects encountered in subsonic compressor designs should have little effect on the blade-element efficiency. The theory is similar to that presented in reference 2, but the efficiency for a single blade row based on static-pressure rise is used instead of the efficiency for the entire stage and the higher-order terms in drag-lift ratio D/L are included. It is shown in appendix A that the blade-element efficiency for a blade row is given by

$$\eta_{st,i} = \frac{1 - \frac{1}{w_m}\frac{D}{L}}{1 + w_m\,(D/L)} \tag{10}$$

or

$$\eta_{st,i} = \frac{\tan\,(90^\circ - \beta_m)}{\tan\,(90^\circ - \beta_m + \epsilon)} \tag{11}$$

which, as might be expected, is the same as the profile efficiency of a propeller.

The variation of the blade-element efficiency with ratio of the mean whirl velocity to axial velocity w_m is shown in figure 5 for values of D/L of 0, 0.05 and 0.10. For optimum angles of attack and efficient blading, the value of D/L should be less

than 0.05 and high blade-element efficiencies should therefore be obtained. Because of the large variations in axial velocity, the large and complex secondary flow, and the frictional effects of the walls, the blade-element analysis probably gives an inaccurate representation for the efficiency in the region of the blade root and blade tip.

Because the analysis applies to either rotor or stator blades, the optimum value of w_m is the same for each, and the resulting optimum velocity diagram for the stage is symmetrical. For a symmetrical velocity diagram, the losses and the ideal pressure rises are the same for the rotor and stator blades (assuming that differences in the boundary-layer conditions do not affect the value of D/L), and the efficiency of conversion to static pressure for the stage is the same as for each blade row; consequently, figure 5 also represents the stage efficiency for a symmetrical diagram. The efficiency for a symmetrical velocity diagram (fig. 5) differs slightly from that given in reference 2 because of the inclusion of the higher-order terms in D/L. For a nonsymmetrical velocity diagram, the blade-element efficiency for the stage is the weighted average of the blade-element efficiencies for the rotor and stator blades with the weighting factor given by the ideal pressure rise of each. The relations derived in the present analysis should be accurate over a wide range of values of D/L and w_m. Because the curves of figure 5 are fairly flat in the region of peak efficiency, a moderate deviation from the optimum value of w_m produces only a small loss in blade-element efficiency.

Blade-Element Pressure Ratio

General considerations. - If radial flow is neglected, the pressure ratio across a row of blades, either rotor or stator, is given by

$$\frac{p_2}{p_1} = \left\{1 + \frac{\gamma-1}{2} M_1^2 \left[1 - \left(\frac{V_2}{V_1}\right)^2\right]\right\}^{\frac{\gamma \eta_p}{\gamma-1}} \tag{12}$$

which is obtained from equations (2), (3), and (9). For a given value of γ, the pressure ratio thus depends only on the inlet Mach number M_1, the velocity ratio V_2/V_1, and the polytropic efficiency η_p. If the efficiency could be held constant, very high pressure ratios obviously could be obtained by increasing the Mach number. With conventional compressor designs, it has been found, however, that the

efficiency drops very rapidly if the inlet Mach number is increased much beyond the critical Mach number of the blades. For this reason designs for entrance Mach numbers appreciably above the critical Mach number of the blades have generally been considered impractical. Kantrowitz has shown, however, that, with suitable design, supersonic relative inlet velocities can be employed to obtain high pressure ratios without serious loss in efficiency (reference 7).

With given Mach number and efficiency, equation (12) shows that the pressure ratio increases as the velocity ratio V_2/V_1 decreases, but at a continuously decreasing rate, and reaches a maximum at a velocity ratio of 0. Not all of the static-pressure rise resulting from a decrease in the relative velocity, however, represents a gain in the total-pressure ratio of the compressor. Only changes in the whirl component of velocity are effective in increasing the total pressure. Although the total pressure is increased only across the rotor blades, the stator blades generally must change the whirl component of velocity by the same amount in the opposite direction in order that the process can be repeated in the next stage. Changes in the axial component of velocity have no direct effect on the total-pressure ratio obtained.

The possibility of an indirect effect on the total-pressure ratio must, however, be considered. Schicht proposed increasing the total pressure ratio by using a rapidly increasing axial component of velocity through the rotor (reference 3). The argument for this procedure is that, when the usual adverse pressure gradient is avoided, a larger change in tangential velocity and hence a greater total-pressure ratio can be obtained. This method may be effective for single-stage, low-speed blowers in applications where high discharge velocity is desired. The method is unsuitable, however, for high-speed, multistage axial-flow compressors, because, in order to be able to repeat the process in a number of stages, the axial velocity has to be again reduced through the stator blades. The argument that an increasing axial velocity makes possible a large change in whirl velocity suggests that it would be very difficult to obtain with reasonable efficiency the required change in whirl velocity in the stators, where the axial velocity is decreasing. Excessively high Mach numbers at the inlet to the stators are also encountered if reasonable rotor speeds and inlet Mach numbers to the rotor blades are used.

The reverse procedure, in which the axial velocity is decreased across the rotor, has been used in a supersonic compressor described in reference 7. This procedure may be desirable for supersonic designs, but for subsonic designs with definite Mach-number

limitations, which are hereinafter considered, little is to be gained in increased pressure ratio by appreciable changes in axial velocity across any blade row. A gradual change in the axial velocity through a multistage compressor may be desirable to obtain favorable conditions at the inlet to each stage, but any increase in total-pressure ratio that is obtained results principally from the more favorable inlet conditions to the succeeding stages rather than from the direct effect of change in axial velocity across a stage. In analyzing the blade-element performance of a single stage in relation to its effect on the total-pressure ratio of the compressor, the actual stage can therefore be replaced by an equivalent stage with the same entrance Mach number and changes in tangential velocity but with constant axial velocity. Because the static-pressure ratio across such an equivalent stage is practically the same as the total-pressure ratio, the consideration of static-pressure ratios alone is sufficient.

Pressure ratio based on constant axial velocity. - For constant axial velocity the velocity ratio across a blade row is given by

$$\frac{V_2}{V_1} = \frac{\cos \beta_1}{\cos \beta_2}$$

and hence from equation (12) the pressure ratio is

$$\frac{p_2}{p_1} = \left\{1 + \frac{\gamma-1}{2} M_1^2 \left[1 - \left(\frac{\cos \beta_1}{\cos \beta_2}\right)^2\right]\right\}^{\frac{\gamma \eta_p}{\gamma-1}} \tag{13}$$

The minimum possible value of the velocity ratio for a given inlet-air angle β_1 is equal to the cosine of the inlet-air angle. For constant axial velocity, the inlet-air angle must thus be large to obtain appreciable diffusion through any row of blades.

The actual pressure ratio that can be obtained, however, depends also on the practical limitations on the turning of the air. The usual limitations are based on blade lift coefficient C_L and solidity σ. (See references 2, 8, p. 39, and 9.) The relation between lift coefficient, solidity, and air angles is given (see appendix A) by

$$C_L \sigma = \frac{2 \cos \beta_m (\tan \beta_1 - \tan \beta_2)}{1 + (D/L) \tan \beta_m} \tag{14}$$

A graphical representation based on these relations showing $C_L\sigma$ as a function of inlet-air angle and turning angle for the case of D/L equal to 0 is shown in figure 6. For most practical applications the term $(D/L) \tan \beta_m$ can be neglected but if high accuracy is desired, the effect of drag can be taken into account by dividing the value of $C_L\sigma$ obtained from figure 6 by $1 + (D/L) \tan \beta_m$. The pressure ratio, expressed in terms of the ratio w_m of mean tangential velocity to the axial velocity, is given by

$$\frac{p_2}{p_1} = \left[1 + (\gamma-1) M_1^2 \frac{w_m(-\Delta w)}{1 + \left(w_m - \frac{\Delta w}{2} \right)^2} \right]^{\frac{\gamma \eta_p}{\gamma - 1}} \tag{15}$$

The value of $-\Delta w$ in terms of $C_L\sigma$ is

$$-\Delta w = \frac{1}{2} C_L\sigma \sqrt{1 + w_m^2} \left[1 + w_m \left(\frac{D}{L} \right) \right] \tag{16}$$

(See appendix A for derivation of relations.)

The pressure ratio as a function of w_m for $M_1 = 0.7$ and $C_L\sigma = 1$ for three values of D/L is shown in figure 7(a). The polytropic efficiency was assumed equal to the efficiency for incompressible flow given by equation (10). For the isentropic case (D/L = 0), the pressure ratio increases asymptotically to a maximum as w_m increases but is very near the maximum value at $w_m = 4$. As the value of D/L is increased, the maximum pressure ratio is obtained at progressively lower values of w_m because of the drop in efficiency when w_m is increased beyond 1 (fig. 5). Even with a value of D/L of 0.10, the maximum pressure ratio occurs at a value of w_m more than twice that for maximum efficiency. The effect of $C_L\sigma$ on the pressure ratio is shown in figure 7(b).

The variation in pressure ratio with w_m shown in figures 7(a) and 7(b) is quite different from the familiar variation (references 8, pp. 99-105, and 10) when the rotor speed instead of the relative inlet Mach number is constant. The variation in pressure ratio with w_m for a symmetrical velocity diagram when the ratio of blade speed to inlet velocity of sound U/a_1 is constant at 0.5 and the value of D/L is 0.05 is shown in figure 7(c) with the inlet relative Mach number M_1 shown as contours. The increase

in pressure ratio with decreasing w_m is due to the large increase in relative Mach number for small values of w_m. The actual attainment of the pressure ratios indicated in figure 7(c) for high values of M_1 is, of course, very doubtful because of the difficulty of maintaining the same value of D/L as for the low values of M_1. The curves are, however, significant in indicating the trend of the pressure ratio over any range of values of w_m in which D/L can be maintained substantially constant. The range of values of w_m over which D/L can be readily maintained at a value comparable to that given in figure 7(c) depends upon the value of U/a_1, but the general trend of the curves is essentially the same for different values of U/a_1. The important conclusion to be drawn from figure 7(c) is that, for a given rotor speed, the pressure ratio can be increased by increasing the design axial velocity up to the point where the effect of increased blade drag resulting from compression shock counterbalances the direct effect of increased Mach number.

Although limitations based on $C_L\sigma$ are widely used in fan and compressor design, it is not always realized that these limitations vary with the value of w_m and hence with the blade stagger. Unfortunately, only meager experimental data on this important point are available. According to Howell in an unpublished British report, the allowable value of C_L drops appreciably with increasing values of w_m, and $-\Delta w$ (equal to $\tan \alpha_1 - \tan \alpha_2$ in Howell's notation) is a better limitation at values of w_m less than unity. The pressure ratio is shown in figure 7(d) for a constant value of $-\Delta w = 0.7424$ (corresponding to its value for $C_L\sigma = 1$; $w_m = 1$), both for a constant value of M_1 and for a constant value of U/a_1. The available data seem to indicate that, when the value of w_m is less than unity, the limitation based on $-\Delta w$ is preferable, whereas, at values of w_m greater than unity, the limitation based on $C_L\sigma$ is better. On the basis of either of these limitations on the turning of the air, for a given inlet Mach number a considerable drop in pressure ratio occurs if w_m is decreased much beyond 1.

The preceeding analysis has shown that, for reasonable limitations on the turning of the air, the pressure ratio increases with the inlet Mach number when either the value of w_m or the value of U/a_1 is held constant. The Mach number thus plays a dominant role in determining the pressure ratio. In order to obtain high pressure ratios per stage, a compressor should therefore be designed for a velocity distribution that gives as nearly as possible the limiting relative Mach number at the entrance to all blade elements.

Specific Mass Flow

The mass flow through a unit cross-sectional area of a compressor is given by

$$\frac{W}{A} = g\rho_T a_T \frac{M \cos \beta}{\left[1 + \frac{\gamma-1}{2} M^2\right]^{\frac{\gamma+1}{2(\gamma-1)}}} \tag{17}$$

where the quantities M and β are with respect to an absolute reference frame. (See appendix A.) Because both ρ_T and a_T increase through the compressor, the mass flow per unit area for a given absolute Mach number M and flow angle β also increases through the compressor. Only at the compressor inlet does the mass flow per unit area therefore provide an essential limitation on the total mass flow for a compressor of a given diameter. Because this analysis is unconcerned with the effect of variation in inlet conditions, it is sufficient to consider the mass flow per unit area for total pressures and temperatures equal to standard sea-level pressures and temperatures. This flow is referred to hereinafter as "specific mass flow". The specific mass flow for dry air with γ equal to 1.4 is given by (see appendix A)

$$\frac{W\sqrt{\theta}}{\delta A} = \frac{85.4 M \cos \beta}{(1 + 0.2 M^2)^3} \tag{18}$$

The maximum specific mass flow is obtained when $\beta = 0$ and $M = 1$ and is equal to 49.4 pounds per second per square foot. For this condition to occur ahead of the first rotor, the inlet Mach number relative to the first rotor must be supersonic. The decrease in specific mass flow for a moderate change in M or β from the optimum values, however, is slight. For example, for a value of M of 0.7, the reduction in specific mass flow is only 9 percent.

For a subsonic compressor design with a given Mach-number limitation and rotor speed, the maximum specific mass flow is obtained with an approximately symmetrical velocity diagram, because any appreciable deviation from symmetry requires a substantial reduction in axial velocity to keep within the Mach-number limitation on both the rotor and stator blades. For a symmetrical velocity diagram and a relative inlet Mach number $M_{1,R}$ the specific mass flow is given by

$$\frac{W\sqrt{\theta}}{\delta A} = \frac{85.4\ M_{1,R}}{\left[1 + 0.2\ M_{1,R}^{2}\ \frac{1 + \left(w_m + \frac{\Delta w}{2}\right)^2}{1 + \left(w_m - \frac{\Delta w}{2}\right)^2}\right]^3 \sqrt{1 + \left(w_m - \frac{\Delta w}{2}\right)^2}} \qquad (19)$$

The variation of the specific mass flow with w_m is shown in figure 8 for a symmetrical velocity diagram with given Mach number and $C_L\sigma$ limitations. The maximum specific mass flow is obtained at low values of w_m but the rate of increase becomes very small as w_m is decreased below 0.4. At a value of w_m equal to 1, corresponding to the maximum blade-element efficiency, the specific mass flow is about 70 percent of its maximum value.

APPLICATION OF BLADE-ELEMENT THEORY TO COMPRESSOR DESIGN

Efficiency

The blade-element theory applies to the main portion of the annular passage; the flow near the ends of the blades must be separately considered. The friction of the annular walls and the secondary flow near the blade ends reduces the efficiency below the values based on blade-element efficiency alone.

In an analysis based on compressor data, Howell (reference 11) has expressed these losses as drag coefficients that are to be added to the profile drag coefficient to obtain the total drag coefficient of the blade. These drag coefficients are given by

$$C_{D,an} = 0.020\ S/l \qquad (20)$$

for the annulus losses and by

$$C_{D,s} = 0.018\ C_L^2 \qquad (21)$$

for the secondary-flow losses. Because the method of treatment when the velocity diagram varies appreciably from hub to tip is not indicated by Howell and because his basis for analyzing profile efficiency

is different from that presented in this report, the empirical equations (20) and (21) indicate only in a qualitative way how the performance based on blade-element efficiency is modified by these additional losses.

The main effect of these additional losses would appear to be an increase in the effective drag-lift ratio without materially affecting the velocity-diagram relations developed in the blade-element theory. The blade-element theory can therefore be used to obtain an indication of the effect of different velocity distributions on the compressor efficiency. In estimating the over-all polytropic efficiency of a compressor, the efficiency of each blade element must be weighted in proportion to the product of the mass flow over that blade element and the ideal pressure rise across the blade element. Although it is impractical to maintain the theoretical optimum value of $w_m = 1$ for all blade elements in a compressor, in the final choice of the velocity distribution for a compressor, the effect of deviations from the optimum value of w_m on the over-all efficiency should be considered. As shown in figure 5, however, the decrease in over-all efficiency for moderate deviations from the optimum value of w_m is inappreciable.

The blade-element theory shows that, to obtain an increase in blade-element efficiency, research must be directed toward the reduction of drag-lift ratio rather than a reduction of drag alone. The over-all efficiency depends also to a considerable extent on the losses associated with secondary flow not considered in the blade-element theory. In order to obtain a substantial reduction in secondary-flow losses, a much more detailed analysis of the three-dimensional flow than that given by the blade-element theory is therefore required.

Compressor Size

The blade-element theory shows for subsonic designs the possibility of decreasing both the diameter and the length of a compressor for a given air flow and pressure ratio by careful consideration of the velocity distribution. A superficial consideration of figures 7(b) and 8 would suggest that for constant relative Mach number any effort to reduce the diameter by decreasing w_m in order to increase the specific mass flow would of necessity decrease the pressure ratio per stage and thereby increase the compressor length. This argument, however, considers only a single blade element and neglects the actual limitations that occur in a

multistage compressor. First, once the rotor speed is fixed for any reason, the pressure ratio across a blade element can be increased by decreasing the value of w_m to the point where the limiting Mach number is reached as shown by figure 7(c). Second, the specific mass flow limits the mass flow of the compressor only at the inlet to the compressor. Because the inlet stage tends to limit both the mass flow and the rotor speed of a compressor, the consideration of velocity distribution in the inlet stage is particularly important.

A small hub-tip diameter ratio at the inlet is desirable for high mass flow through a given diameter. For the conventional type of axial-flow stage, ratios much below 0.5 appear impractical although lower values might possibly be used in a very high-solidity stage with considerable hub taper.

Velocity distribution in inlet stage. - The method of design based upon free-vortex flow is widely used because of the simplicity and the relatively high accuracy with which the flow can be calculated. The velocity diagrams for a free-vortex design for high specific mass flow with a hub-tip diameter ratio of 0.55 is shown in figure 9(a). For simplicity, the effect of passage taper is neglected. The maximum pressure ratio compatible with this type of design was obtained by making the maximum Mach number the same (0.7) on the rotor and stator blades. The maximum Mach number occurs at the tip on the rotor blades and at the hub on the stator blades.

The blade-element theory shows that this type of design has several disadvantages. The velocity diagram is unsymmetrical at all but one radius and the inlet Mach number for most of the blade length is much below the limiting value. The result is a rather low pressure ratio per stage. At the hub the relative velocity at the exit of the rotor is actually greater than at the inlet. There is some question whether the flow would actually start in the direction indicated. This uncertainty of flow direction can be eliminated by making the velocity diagram more symmetrical at the hub but the pressure ratio of the stage is reduced further by this adjustment.

The use of a symmetrical velocity diagram with constant total enthalpy at all radii (fig. 9(b)), which may be obtained by properly designed entrance guide vanes, eliminates these disadvantages. The same Mach-number and $C_L\sigma$ limitations are used as for the free-vortex design. The principal difference is that the entrance Mach number is very nearly constant for all blade elements of both rotor and stator blades. The inlet Mach number at the hub is actually slightly higher than at the tip because of the increase in axial

velocity toward the hub for this type of rotation. The specific mass flow is also somewhat higher for the symmetrical velocity diagram than for a free vortex because of the increase in axial velocity toward the hub. A comparison of the specific mass flow and pressure ratio for the two types of velocity distribution with the same maximum inlet Mach number for each is shown in the following table:

	$W\sqrt{\theta}/\delta A$	$\Delta p/p_1$	$\frac{\Delta p \text{ (vortex)}}{\Delta p \text{ (symmetrical diagram)}}$
Symmetrical diagram	37.4	0.136	
Free vortex, same $(C_L\sigma)_h$	35.1	.087	0.64
Free vortex, same $-\Delta w_h$	35.2	.091	.67

Limitations on turning based on both $C_L\sigma$ and on Δw are shown. The limitations are conservative but are the same for both types of design and should therefore give the relative, but not necessarily the maximum, performance for the two designs. Not only is the pressure ratio for the inlet stage higher for the symmetrical diagram than for the vortex but also the pressure ratio obtainable in the succeeding stages is higher because of a higher rotor speed allowed for the symmetrical-design diagram (12 percent higher in this case).

A disadvantage of the design based on symmetrical velocity and constant total enthalpy is that the axial velocity may become very low or actually reverse near the tip, especially after the rotor, for low mass flow. The decrease in axial velocity across the rotor blades at the tip is not shown in the velocity diagram. The variation in axial velocity from hub to tip serves a useful purpose in producing a more uniform entrance Mach number but, if too large, results in flow separation along the outer wall. The magnitude of the radial variation in axial velocity for the symmetrical-diagram design is a function of w_m at some particular radius, such as the hub, and increases with increasing values of w_m. The axial velocity at the casing may become 0 if the value of w_m at the hub is made much greater than the value used in this example. The design based on a symmetrical velocity diagram and constant total enthalpy along the radius is therefore suitable only for designs with high specific mass flow. A velocity distribution somewhere between a free vortex and a symmetrical velocity diagram at all radii would probably be preferable for designs of lower specific mass flow than that considered in the example of

figure 9(b). Small variations in the total enthalpy along the radius may also be useful in obtaining more suitable velocity diagrams in later stages. The determination of the theoretical optimum distribution of velocity and enthalpy is very complex because of the infinite number of possible variations, but a good approximation to an optimum design for given conditions is possible with the aid of the blade-element theory.

Axial variations through compressor. - The blade-element theory is also very useful in the analysis of the effect of different variations of axial velocity from stage to stage. The speed of the rotor is usually determined by the Mach-number limitation on the first row of rotor blades. For maximum pressure ratio per stage, an increase in the blade velocity U in the later stages would be desirable. In the usual designs, the angular velocity of all the rotor blades is the same because they are mounted on the same shaft. The blade-element velocity U, however, can be increased by increasing the radial distance from the axis. The increase in the tip diameter, however, increases the over-all diameter of the compressor for a given specific mass flow at the compressor inlet. If a larger over-all diameter is to be used, the use of the larger diameter also at the inlet would appear desirable in order to allow a higher hub-tip diameter ratio with a given mass flow. The increase in the tip diameter in the later stages therefore is of dubious value.

The increase in hub diameter from stage to stage, however, produces a higher pressure ratio per stage both by increasing the blade-element velocity at the hub U_h and by maintaining the inlet Mach number near the limiting value by an increase in axial velocity (fig. 7(c)). The maximum pressure ratio with a constant casing diameter is obtained by increasing the hub diameter from stage to stage in such a manner as to obtain the limiting Mach number on each stage. Because the velocity of sound increases, the axial velocity at the casing must be increased to maintain the same Mach number. For pressure ratios of 5 or more, this procedure leads to very short blades and high ratios of hub to tip diameter in the last stages. The tip-clearance losses will be increased, unless the absolute clearances are reduced, because of the greater relative clearance for the short blades. The annulus losses may also be a larger percentage of the energy input because of higher ratio of passive, or annulus, area to active, or blade, area (reference 12). The use of small blade chords will reduce this ratio of passive to active area as well as reduce the length of the compressor, but the adverse effect of reducing the Reynolds number must be considered (reference 12). Because of the relatively high density and velocity

in the last stages, however, the chords can be made considerably smaller than in the inlet stages and the same Reynolds number maintained. The diffuser requires more careful attention with high axial velocities at the compressor outlet but the diffuser losses become less important as the over-all pressure ratio is increased. The use of boundary-layer control, even for high outlet velocities, should make it possible to obtain efficient diffusion in a very short diffuser (reference 13). The required suction should not be difficult to provide. For example, the boundary-layer air removed might be used for cooling some portion of the turbine where the pressure is lower than that in the diffuser.

The high losses reported by Eckert (reference 12) for high hub-tip diameter ratios in single-stage blowers appear to be less serious in multistage compressors. The hub-tip diameter ratio is quite high in the last few stages of the NACA eight-stage axial-flow compressor (0.93 in the last stage). (See reference 2.) Although no information is available on the efficiency of the last stages, the over-all efficiency (references 1, 2, and 14) is much higher than would be expected if the efficiency dropped off as indicated by Eckert.

Flexibility and Range

Very little has yet been done on the investigation of the effect of design variables on the range and the flexibility of axial-flow compressors. An unpublished British report made a theoretical analysis based on cascade data of several types of design, but the differences in range for practical designs were not particularly remarkable. The problem of range and flexibility is considered from an entirely different point of view in reference 1, where the possible extension of the useful range by the use of adjustable stator blades is investigated. Improvements in the efficiency at other than design speed and a considerable extension of the flow range at any given speed were found to be possible by the adjustment of the stator blades alone. An improvement of about 0.08 in efficiency over the design setting for one of the blade resettings at approximately half the design speed was obtained. A shift of the peak-efficiency flow by 20 to 30 percent was possible over the entire speed range by the use of different stator-blade settings. The extension in the flow range was particularly striking at a compressor Mach number of 0.8 because of the very narrow range at this speed with any one blade setting. An approximately sevenfold increase in the flow range was obtained at this compressor speed by the use of different stator-blade settings.

The success of this method in extending the useful range of axial-flow compressors has warranted the development of a more rapid method for computing blade resettings than that presented in reference 1. Figures 3, 4, and 6 provide the basis for such a method, as is illustrated by the example in appendix B.

SUMMARY OF ANALYSIS

A blade-element theory developed for analyzing the effect of basic design variables on axial-flow-compressor performance may be summarized as follows:

The one-dimensional compressible-flow theory shows that the effect of polytropic efficiency on the flow relations across a row of blades is of the same order of magnitude as the effect of the Mach number. Flow calculations based upon isentropic compressible flow may therefore be appreciably in error. The blade-element efficiency based on static-pressure rise and the assumption of incompressible flow in terms of drag-lift ratio and mean flow angle is shown to be the same as the profile efficiency of a propeller. For substantial improvement in compressor efficiency, research should be directed toward a reduction in blade-element drag-lift ratio and toward a better understanding of secondary-flow phenomena.

The relative Mach number is shown to be a dominant factor in determining the pressure ratio and, if the efficiency can be maintained, very high pressure ratios per stage are possible with supersonic designs. But even for subsonic compressor designs, considerable increase in pressure ratio over that for conventional designs can be obtained by producing a velocity distribution that gives relative inlet Mach numbers close to the limiting Mach number on all blade elements. With a given inlet Mach number, the pressure ratio obtainable across a blade row increases and the specific mass flow decreases as the ratio of mean whirl velocity to axial velocity increases for the high-efficiency range of this velocity ratio. For subsonic compressor designs with a definite Mach-number limitation, the velocity distribution in the inlet stage is particularly important because the inlet stage limits both the mass flow and the rotor speed of the compressor and thereby limits the pressure ratio of later stages as well as the inlet stage. By the use of entrance guide vanes designed to produce a variable axial velocity at the entrance to the first rotor, a substantial increase in stage pressure

ratio and a slight increase in the specific mass flow over designs based on free vortex with the same Mach-number and turning limitations are shown to be possible. In the succeeding stages, the maximum pressure ratio per stage without an increase in compressor diameter is obtainable by increasing the hub diameter to obtain the maximum axial velocity compatible with the Mach-number limitation.

Flight Propulsion Research Laboratory,
National Advisory Committee for Aeronautics,
Cleveland, Ohio.

APPENDIX A

DERIVATION OF EQUATIONS

Adiabatic and polytropic efficiencies. - For different ideal reversible processes, such as adiabatic, isothermal, and polytropic, the densities will be different functions of the pressure and by equation (7) the efficiencies obtained will be different. Because most actual compression processes are approximately adiabatic, the efficiency based on a reversible adiabatic process as the ideal process has been widely used. The polytropic efficiency is also useful because it is equal to the efficiency of the individual small stages of an adiabatic compression when the efficiency of these small stages is constant throughout. For this reason, it is often referred to as "small-stage" efficiency. For constant specific heat, the density is given by

$$\rho = \rho_1 \left(\frac{p}{p_1}\right)^{\frac{1}{\gamma}} \tag{22}$$

for the reversible adiabatic process and by

$$\rho = \rho_1 \left(\frac{p}{p_1}\right)^{\frac{1}{m}} \tag{23}$$

for the polytropic process. The polytropic exponent m for the ideal process is chosen to give the same density and temperature at the final pressure p_2 as for the actual process. The substitution of these expressions in equation (7) and the use of the perfect gas law gives the following values for the adiabatic and polytropic efficiencies

$$\eta_{ad} = \frac{gRt_1 \frac{\gamma}{\gamma-1}\left[\left(\frac{p_2}{p_1}\right)^{\frac{\gamma-1}{\gamma}} - 1\right]}{\Delta h} \tag{24}$$

$$\eta_p = \frac{gRt_1 \frac{m}{m-1}\left[\left(\frac{p_2}{p_1}\right)^{\frac{m-1}{m}} - 1\right]}{\Delta h} \tag{25}$$

The thermodynamic relations

$$\Delta h = Jgc_p (t_2 - t_1) = gR \frac{\gamma}{\gamma-1} (t_2 - t_1) \tag{26}$$

and

$$\left(\frac{p_2}{p_1}\right)^{\frac{m-1}{m}} = \frac{t_2}{t_1} \tag{27}$$

when substituted in equations (24) and (25) give

$$\eta_{ad} = \frac{\left(\frac{p_2}{p_1}\right)^{\frac{\gamma-1}{\gamma}} - 1}{\frac{t_2}{t_1} - 1} \tag{28}$$

or

$$\eta_{ad} = \frac{\left(\frac{p_2}{p_1}\right)^{\frac{\gamma-1}{\gamma}} - 1}{\left(\frac{p_2}{p_1}\right)^{\frac{m-1}{m}} - 1}$$

and

$$\eta_p = \frac{m/(m-1)}{\gamma/(\gamma-1)} \tag{29}$$

Therefore

$$\eta_{ad} = \frac{\left(\frac{p_2}{p_1}\right)^{\frac{\gamma-1}{\gamma}} - 1}{\left(\frac{p_2}{p_1}\right)^{\frac{\gamma-1}{\gamma\eta_p}} - 1} \tag{8}$$

which is equation (8) of this report. By the use of L'Hospital's rule, the limiting value of η_{ad} as p_2/p_1 approaches 1 can readily be shown to be equal to η_p.

If equation (29) is solved for m, the polytropic exponent is given as a function of the polytropic efficiency

$$m = \frac{\eta_p}{\eta_p - \frac{\gamma-1}{\gamma}} \tag{9}$$

Although the derivations have been made in terms of static pressures, temperatures, and enthalpies, all the relations used apply equally well to total states; the values of the efficiencies and the polytropic exponents for a particular compressor will, of course, be somewhat different.

Pressure ratios. - The pressure ratio across a row of blades for constant axial velocity can be expressed in terms of w_m, $-\Delta w$, and M by use of equation (12) and figure 1(b)

$$\frac{p_2}{p_1} = \left(1 + \frac{\gamma-1}{2} M_1^2 \frac{V_1^2 - V_2^2}{V_1^2}\right)^{\frac{\gamma\eta_p}{\gamma-1}}$$

$$= \left(1 + \frac{\gamma-1}{2} M_1^2 \frac{V_a^2}{V_1^2} \frac{V_{w,1}^2 - V_{w,2}^2}{V_a^2}\right)^{\frac{\gamma\eta_p}{\gamma-1}}$$

$$= \left[1 + (\gamma-1) M_1^2 \frac{V_a^2}{V_1^2} \frac{V_{w,1} + V_{w,2}}{2V_a} \frac{V_{w,1} - V_{w,2}}{V_a}\right]^{\frac{\gamma\eta_p}{\gamma-1}}$$

$$= \left[1 + (\gamma-1) M_1^2 \frac{w_m(-\Delta w)}{1 + \left(w_m - \frac{\Delta w}{2}\right)^2}\right]^{\frac{\gamma\eta_p}{\gamma-1}} \tag{15}$$

Blade-element efficiency. - A blade-element efficiency for incompressible flow based on the power input to the air by the rotor is suitable if applied to an entire stage, as in reference 2, but is not suitable for considering the performance of a single blade row. For flow across a single blade row with no change in radius,

$$\Delta h = \frac{V_1^2}{2} - \frac{V_2^2}{2} \tag{30}$$

and the general expression for efficiency based on static states (equation (7)) becomes, for the case of incompressible flow considered here,

$$\eta_{st,i} = \frac{\Delta p}{\frac{\rho V_1^2}{2} - \frac{\rho V_2^2}{2}} \tag{31}$$

which is the usual simplified expression for diffuser efficiency in which velocity variations across the passage are neglected (reference 15).

For constant axial velocity, the following relations can readily be obtained from figure 10 and momentum considerations

$$\Delta p = \frac{F_a}{S} = \frac{1}{S}\left(L \sin \beta_m - D \cos \beta_m\right)$$

$$= \frac{L \sin \beta_m}{S}\left(1 - \frac{D}{L} \cot \beta_m\right) \tag{32}$$

$$L = \frac{F_\theta - D \sin \beta_m}{\cos \beta_m}$$

$$= \frac{F_\theta}{\cos \beta_m} - L \frac{D}{L} \tan \beta_m$$

or by solving for L

$$L = \frac{F_\theta}{\cos \beta_m \left[1 + (D/L) \tan \beta_m\right]}$$

$$= \frac{\rho V_a^2 S (\tan \beta_1 - \tan \beta_2)}{\cos \beta_m \left[1 + (D/L) \tan \beta_m\right]} \tag{33}$$

If this lift is substituted in equation (32),

$$\Delta p = \frac{\rho V_a^2 \tan \beta_m (\tan \beta_1 - \tan \beta_2) \left[1 - (D/L) \cot \beta_m\right]}{1 + (D/L) \tan \beta_m}$$

$$= \frac{\rho V_a^2 w_m (-\Delta w) \left[1 - \frac{1}{w_m}\left(\frac{D}{L}\right)\right]}{1 + w_m (D/L)} \tag{34}$$

also

$$\frac{\rho V_1^2}{2} - \frac{\rho V_2^2}{2} = \frac{\rho}{2} (V_{w,1}^2 - V_{w,2}^2)$$

$$= \rho V_a^2 w_m (-\Delta w) \tag{35}$$

By the substitution of equations (34) and (35) in equation (31), the blade-element efficiency based on static-pressure rise and incompressible flow is finally obtained as

$$\eta_{st,i} = \frac{1 - \frac{1}{w_m}\left(\frac{D}{L}\right)}{1 + w_m (D/L)} \tag{10}$$

The blade-element efficiency can also be expressed in terms of the "gliding angle" ϵ (fig. 10), which is defined by

$$\tan \epsilon = D/L \tag{36}$$

The profile efficiency is

$$\eta_{st,i} = \frac{\tan (\beta_m - \epsilon)}{\tan \beta_m}$$

$$= \frac{\tan (90^\circ - \beta_m)}{\tan (90^\circ - \beta_m + \epsilon)} \qquad (11)$$

which is the same as the expression for the profile efficiency of a propeller.

Lift coefficient. - The relations for $C_L\sigma$, equations (22) and (23) of reference 1, neglect the effect of drag and give the values corresponding to $D/L = 0$. The exact expressions, for values of D/L different from 0, can readily be derived from equations (2) and (6) of reference 1

$$F_\theta = \rho S V_a^2 (-\Delta w)$$

and

$$L = \frac{F_\theta}{\cos \beta_m [1 + (D/L) \tan \beta_m]}$$

Hence

$$L = \frac{\rho S V_a^2 (-\Delta w)}{\cos \beta_m [1 + (D/L) \tan \beta_m]} = \frac{\frac{\rho c V_a^2}{\sigma} (\tan \beta_1 - \tan \beta_2)}{\cos \beta_m [1 + (D/L) \tan \beta_m]}$$

and the value of $C_L\sigma$ is obtained by multiplying by $\frac{2\sigma}{\rho V_m^2 c}$.

$$C_L\sigma = \frac{L\sigma}{\frac{1}{2}\rho V_m^2 c} = \frac{2V_a^2 (\tan \beta_1 - \tan \beta_2)}{V_m^2 \cos \beta_m [1 + (D/L) \tan \beta_m]}$$

$$= \frac{2 \cos \beta_m (\tan \beta_1 - \tan \beta_2)}{1 + (D/L) \tan \beta_m} \qquad (14)$$

This relation can also be expressed in terms of the variables w_m and $(-\Delta w)$ by referring to figure 1(b):

$$C_L\sigma = \frac{-2\Delta w}{\sqrt{w_m^2 + 1}\left[1 + (D/L) w_m\right]}$$

which when solved for $-\Delta w$ becomes equation (16) of the report

$$-\Delta w = \frac{1}{2} C_L \sigma \sqrt{1 + w_m^2} \left(1 + w_m \frac{D}{L}\right) \qquad (16)$$

Specific mass flow. - The mass flow through a unit cross-sectional area in terms of an absolute reference frame is

$$\frac{W}{A} = g\rho V_a$$

$$= g\rho_T a_T \frac{\rho}{\rho_T} \frac{a}{a_T} \frac{V}{a} \cos \beta$$

$$= g\rho_T a_T \frac{M \cos \beta}{\left(1 + \frac{\gamma-1}{2} M^2\right)^{\frac{\gamma+1}{2(\gamma-1)}}} \tag{17}$$

$$= \frac{P\sqrt{\gamma g}}{\sqrt{RT}} \frac{M \cos \beta}{\left(1 + \frac{\gamma-1}{2} M^2\right)^{\frac{\gamma+1}{2(\gamma-1)}}}$$

$$= \frac{P}{p_0} \sqrt{\frac{t_0}{T}} \frac{p_0 \sqrt{\gamma g}}{\sqrt{Rt_0}} \frac{M \cos \beta}{\left(1 + \frac{\gamma-1}{2} M^2\right)^{\frac{\gamma+1}{2(\gamma-1)}}}$$

$$= \frac{\delta}{\sqrt{\theta}} \frac{2116.2\sqrt{1.4 \times 32.174}}{\sqrt{53.345 \times 518.6}} \frac{M \cos \beta}{\left(1 + 0.2 M^2\right)^3}$$

Hence

$$\frac{W\sqrt{\theta}}{\delta A} = \frac{85.4 M \cos \beta}{\left(1 + 0.2 M^2\right)^3} \tag{18}$$

In order to express this result in terms of the relative Mach number and the velocity-diagram parameters for a symmetrical velocity diagram, it must be remembered that the quantities in equation (18) are

for absolute coordinates at the entrance to the rotor (station 1). With the aid of figure 1(b), which is taken to represent the rotor blades, the following substitutions may be made in equation (18):

$$\frac{W\sqrt{\theta}}{\delta A} = \frac{85.4 \dfrac{V_a}{V_{1,R}} \dfrac{V_{1,R}}{a_1}}{\left[1 + 0.2\left(\dfrac{V_{1,R}}{a_1}\right)^2 \left(\dfrac{V_{1,S}}{V_{1,R}}\right)^2\right]^3}$$

$$= \frac{85.4 \dfrac{V_a}{V_{1,R}} M_{1,R}}{\left[1 + 0.2\, M_{1,R}^2 \left(\dfrac{V_{2,R}}{V_{1,R}}\right)^2\right]^3}$$

$$= \frac{85.4\, M_{1,R}}{\left[1 + 0.2\, M_{1,R}^2 \dfrac{1 + \left(w_m + \dfrac{\Delta w}{2}\right)^2}{1 + \left(w_m - \dfrac{\Delta w}{2}\right)^2}\right]^3 \sqrt{1 + \left(w_m - \frac{\Delta w}{2}\right)^2}} \qquad (19)$$

The value of $-\Delta w$ is given in terms of $C_L\sigma$ by equation (16).

APPENDIX B

EXAMPLE OF USE OF CHARTS FOR COMPUTATION OF STATOR-BLADE RESETTING

The method of computing the stator-blade resetting for different operating conditions given in reference 1 involves considerable labor in the trial-and-error solution of the velocity-ratio equation (equation (19) of reference 1). The charts given in figures 3, 4, and 6 greatly facilitate the computation of stator-blade resetting, as is illustrated by the following example:

The computations are made for a typical stage of the NACA eight-stage axial-flow compressor for an air flow and speed appreciably below the design values. The conditions at the inlet to the stage are determined by the flow from the previous stage and, for the purpose of this example, are assumed to be known. The stage is here taken as a row of stator blades followed by a row of rotor blades. The station designations are: 1, at inlet to stator blades; 2, between stator and rotor blades; and 3, at outlet to rotor blades. Quantities that are a function of the radius are taken at midpassage unless otherwise specified. The following geometric characteristics of the stage are given:

$$A_1/A_2 = 1.118, \quad A_2/A_3 = 1.127$$

$$\psi_S = 45.3^\circ, \quad \psi_R = 43.1^\circ \text{ (design values)}$$

$$\alpha_{a,o} = -5.6^\circ \text{ (for blades used)}$$

$$\sigma_S = 0.9961, \quad \sigma_R = 1.0156$$

$$r_2/r_{2,t} = 0.9004$$

The given inlet conditions and rotor speed are:

$$\beta_1 = 65.3^\circ, \quad V_1/a_1 = 0.492, \quad U_t/a_1 = 0.708$$

It is proposed to reset the stator blades to make the maximum lift coefficient at the mean radius, which may occur on either

the stator or the rotor blades, equal to a prescribed value of 0.8. The adjustment of the stator-blade angle to give a prescribed lift coefficient on the stator blades may be accomplished very simply by the use of figure 6 and the empirical relation from reference 1 (equation (17)):

$$\beta_2 = (1-K)\,\beta_1 + K\psi_S + K\alpha_{a,o}$$

but the lift coefficient on the rotor blades also must be checked in order to determine whether the prescribed maximum is exceeded. If the prescribed maximum lift coefficient is exceeded on the rotor blades, as it is in this example, the lift coefficient must be determined with different stator-blade settings until the prescribed maximum lift coefficient is obtained on the rotor blades. The calculation of the stator-blade setting for a lift coefficient of 0.8 on the stators is first made and the resulting lift coefficient on the rotor blades determined. The calculation for the final trial solution for a lift coefficient of 0.8 on the rotor blades is then presented.

For simplicity, the value of K is assumed to be 0.9 throughout. Somewhat more accurate results could be obtained by estimating the value of K from the values presented in reference 16. A polytropic efficiency η_p of 0.9 is also assumed. The turning angle $\beta_1 - \beta_2$ is found from figure 6 for

$$C_L\sigma = 0.8 \times 0.9961 = 0.797$$

and, for β_1 equal to 65.3°, is 11.5°.

Therefore

$$\beta_2 = 53.8^\circ$$

and from the relation

$$\beta_2 = 0.1\,\beta_1 + 0.9\,\psi_S - 0.9 \times 5.6$$

the value of ψ_S is determined as 58.1°.

The value of C_L for the rotor blades for this stator-blade setting requires the calculation of the flow across the stator. The flow-area ratio is

$$\frac{f_1}{f_2} = \frac{A_1 \cos \beta_1}{A_2 \cos \beta_2} = 1.118\,\frac{\cos 65.3^\circ}{\cos 53.8^\circ} = 0.791$$

By the use of figures 3(c) and 4(c) with $f_1/f_2 = 0.791$ and $V_1/a_1 = 0.492$, the following ratios are obtained: $V_2/V_1 = 0.754$, $t_2/t_1 = 1.021$, and $a_2/a_1 = 1.010$. The flow conditions of the air leaving the stator row may now be obtained from the following relations:

$$\frac{V_2}{a_2} = \frac{V_2}{V_1}\frac{V_1}{a_1}\frac{a_1}{a_2} = \frac{0.754 \times 0.492}{1.010} = 0.367$$

$$\frac{V_{a,2}}{a_2} = \frac{V_2 \cos \beta_2}{a_2} = 0.367 \cos 53.8^\circ = 0.217$$

$$\frac{V_{w,2}}{a_2} = \frac{V_2}{a_2} \sin \beta_2 = 0.367 \cos 53.8^\circ = 0.296$$

$$\frac{U_2}{a_2} = \frac{U_{2,t}}{a_1}\frac{r_2}{r_{2,t}}\frac{a_1}{a_2} = \frac{0.708 \times 0.9004}{1.010} = 0.631$$

The whirl component of the Mach number relative to the rotor is then given by

$$\frac{V_{w,2,R}}{a_2} = \frac{U_2}{a_2} - \frac{V_{w,2,S}}{a_2} = 0.631 - 0.296 = 0.335$$

The air velocity and the air angle relative to the rotor are then obtained from the relations (in which the subscript R has been dropped)

$$\tan \beta_2 = \frac{V_{w,2}/a_2}{V_{a,2}/a_2} = \frac{0.335}{0.217} = 1.544$$

$$\beta_2 = 57.1^\circ$$

$$\frac{V_2}{a_2} = \frac{V_{w,2}/a_2}{\sin \beta_2} = \frac{0.335}{0.840} = 0.399$$

The leaving-air angle may now be obtained from the relation

$$\beta_3 = (1-K)\,\beta_2 + K\psi_R + K\alpha_{a,o}$$

$$= (1-0.9)\ 57.1^\circ + 0.9\ (43.1^\circ) + 0.9\ (-5.6^\circ)$$

$$= 39.5^\circ$$

The flow-area ratio across the rotor row is now obtained from

$$\frac{f_2}{f_3} = \frac{A_2}{A_3}\frac{\cos\beta_2}{\cos\beta_3} = 1.127\ \frac{\cos 57.1^\circ}{\cos 39.5^\circ} = 0.792$$

Using figures 3(c) and 4(c) again with $f_1/f_2 = 0.792$ and $M_1 = 0.399$ (with the obvious changes in subscripts) gives

$$\frac{V_3}{V_2} = 0.770,\quad \frac{t_3}{t_2} = 1.013,\quad \frac{a_3}{a_2} = 1.006$$

and the conditions at the exit of the rotor row are

$$\frac{V_3}{a_3} = \frac{V_3}{V_2}\frac{V_2}{a_2}\frac{a_2}{a_3} = \frac{0.770 \times 0.399}{1.006} = 0.305$$

$$\frac{V_{a,3}}{a_3} = \frac{V_3}{a_3}\cos\beta_3 = 0.305\cos 39.5^\circ = 0.235$$

$$\frac{V_{w,3}}{a_3} = \frac{V_3}{a_3}\sin\beta_3 = 0.305\sin 39.5^\circ = 0.194$$

The turning angle for the rotor row is $\beta_2 - \beta_3 = 57.1^\circ - 39.5^\circ = 17.6^\circ$. Now by use of figure 6, $C_L\sigma = 0.93$, which gives a lift coefficient on the rotor

$$C_L = \frac{0.93}{1.0156} = 0.92$$

This lift coefficient exceeds the maximum allowable value of 0.8. The lift coefficient on the rotor row therefore must be lowered by increasing the stator-blade angles. The stator lift coefficient will also be unavoidably reduced.

After several trials, a value of $\psi_s = 60^\circ$ was found to give approximately the maximum allowable lift coefficient of 0.8 on the rotor blades. The calculations for this case follow:

The turning-angle relation is first applied to find β_2:

$$\beta_2 = (1-K)\,\beta_1 + K\psi_s + K\alpha_{a,o}$$

$$= (1-0.9)\,65.3^\circ + 0.9\,(60^\circ) + 0.9\,(-5.6^\circ)$$

$$= 55.5^\circ$$

The flow-area ratio is

$$\frac{f_1}{f_2} = \frac{A_1 \cos \beta_1}{A_2 \cos \beta_2} = 1.118\,\frac{\cos 65.3^\circ}{\cos 55.5^\circ} = 0.825$$

Using figures 3(c) and 4(c) with $\frac{f_1}{f_2} = 0.825$ and $\frac{V_1}{a_1} = 0.492$ gives

$$V_2/V_1 = 0.792, \quad t_2/t_1 = 1.018, \quad a_2/a_1 = 1.009$$

The conditions leaving the stator row are

$$\frac{V_2}{a_2} = \frac{V_2}{V_1}\frac{V_1}{a_1}\frac{a_1}{a_2} = \frac{0.792 \times 0.492}{1.009} = 0.386$$

$$\frac{V_{a,2}}{a_2} = \frac{V_2}{a_2}\cos \beta_2 = 0.386 \cos 55.5^\circ = 0.218$$

$$\frac{V_{w,2}}{a_2} = \frac{V_2}{a_2}\sin \beta_2 = 0.386 \sin 55.5^\circ = 0.318$$

The conditions at entrance to the rotor row are

$$\frac{U_2}{a_2} = \frac{U_{2,t}}{a_1}\frac{r_2}{r_{2,t}}\frac{a_1}{a_2} = \frac{0.708 \times 0.900}{1.009} = 0.631$$

$$\frac{V_{w,2,R}}{a_2} = \frac{U_2}{a_2} - \frac{V_{w,2,S}}{a_2} = 0.631 - 0.318 = 0.313$$

and relative to the rotor blades

$$\tan \beta_2 = \frac{V_{w,2}/a_2}{V_{a,2}/a_2} = \frac{0.313}{0.218} = 1.435$$

$$\beta_2 = 55.1^\circ$$

$$\frac{V_2}{a_2} = \frac{V_{w,2}/a_2}{\sin \beta_2} = \frac{0.313}{0.820} = 0.382$$

The leaving-air angle β_3 is

$$\beta_3 = (1-K)\ \beta_2 + K\psi_R + K\alpha_{a,o}$$

$$= (1-0.9)\ 55.1^\circ + 0.9\ (43.1^\circ) + 0.9\ (-5.6^\circ)$$

$$= 39.3^\circ$$

The flow-area ratio over the rotor is

$$\frac{f_2}{f_3} = \frac{A_2 \cos \beta_2}{A_3 \cos \beta_3} = 1.127\ \frac{\cos 55.1^\circ}{\cos 39.3^\circ} = 0.833$$

Using figures 4(c) and 5(c) with $f_1/f_2 = 0.833$ and $M_1 = 0.382$ (with the obvious changes in subscripts) now gives

$$V_3/V_2 = 0.810, \quad t_3/t_2 = 1.01, \quad a_3/a_2 = 1.005$$

The flow conditions at the rotor exit may now be obtained:

$$\frac{V_3}{a_3} = \frac{V_3}{V_2}\frac{V_2}{a_2}\frac{a_2}{a_3} = \frac{0.810 \times 0.382}{1.005} = 0.308$$

$$\frac{V_{a,3}}{a_3} = \frac{V_3}{a_3} \cos \beta_3 = 0.308 \cos 39.3^\circ = 0.238$$

$$\frac{V_{w,3}}{a_3} = \frac{V_3}{a_3} \sin \beta_3 = 0.308 \sin 39.3^\circ = 0.195$$

The turning angles for stator and rotor row are

$$\beta_{1,S} - \beta_{2,S} = 65.3^\circ - 55.5^\circ = 9.8^\circ$$

$$\beta_{2,R} - \beta_{3,R} = 55.1^\circ - 39.3^\circ = 15.8^\circ$$

From figure 6 with these turning angles,

$$(C_L\sigma)_S = 0.69$$

$$(C_L\sigma)_R = 0.81$$

The lift coefficients then are

$$C_{L,S} = \frac{0.69}{0.9961} = 0.69$$

$$C_{L,R} = \frac{0.81}{1.0156} = 0.80$$

REFERENCES

1. Sinnette, John T., Jr., and Voss, William J.: Extension of the Useful Operating Range of Axial-Flow Compressors by Use of Adjustable Stator Blades. NACA ACR No. E6E02, 1946.

2. Sinnette, John T., Jr., Schey, Oscar W., and King, J. Austin: Performance of NACA Eight-Stage Axial-Flow Compressor Designed on the Basis of Airfoil Theory. NACA ACR No. E4H18, 1944.

3. Sörensen, E.: Constant-Pressure Blowers. NACA TM No. 927, 1940.

4. Flügge-Lotz, I., and Betz, A.: Design of Centrifugal Impeller Blades. NACA TM No. 902, 1939.

5. Sorg, K. W.: Supersonic Flow in Turbines and Compressors. R.A.S. Jour., vol. XLVI, no. 375, March 1942, pp. 64-85. (From Forschung, vol. 10, no. 6, Nov.-Dec. 1939, pp. 270-285.)

6. Van Driest, E. R.: Steady Turbulent-Flow Equations of Continuity, Momentum, and Energy for Finite Systems. Jour. Appl. Mech., vol. 13, no. 3, Sept. 1946, pp. A231-A238.

7. Kantrowitz, Arthur R.: The Supersonic Axial-Flow Compressor. NACA ACR No. L6D02, 1946.

8. Keller, Curt: The Theory and Performance of Axial-Flow Fans. (Adapted for the use of fan designers by Lionel S. Marks and John R. Weske.) McGraw-Hill Book Co., Inc., 1937.

9. Mutterperl, William: High Altitude Cooling. VI - Axial-Flow Fans and Cooling Power. NACA ARR No. L4I11e, 1944.

10. Bell, E. Barton: Test of a Single-Stage Axial-Flow Fan. NACA Rep. No. 729, 1942.

11. Howell, A. R.: Fluid Dynamics of Axial Compressors. Inst. Mech. Eng. Proc. (British), vol. 153 (War Emergency Issue No. 1), 1945, pp. 441-452.

12. Eckert, B.: The Influence of Physical Dimensions (Such as Hub:Tip Ratio, Clearance, Blade Shape) and Flow Conditions (Such as Reynolds Number and Mach Number) on Compressor Characteristics. Part A - Summary of the Results of Research on Axial Flow Compressors at the Stuttgart Research Institute for Automobiles and Engines, Vol. III, W.A.C. Eng. Trans. No. 22, Wright Aero. Corp., BUSHIPS 338, Navy Dept. (Washington, D.C.), May 1946.

13. Ackeret, J.: Removing Boundary Layer by Suction. NACA TM No. 395, 1927.

14. King, J. Austin, and Regan, Owen W.: Performance of NACA Eight-Stage Axial-Flow Compressor at Simulated Altitudes. NACA ACR No. E4L21, 1944.

15. Patterson, G. N.: Modern Diffuser Design. Aircraft Eng., vol. X, no. 115, Sept. 1938, pp. 267-273.

16. Bogdonoff, Seymour M., and Bogdonoff, Harriet E.: Blade Design Data for Axial-Flow Fans and Compressors. NACA ACR No. L5F07a, 1945.

NATIONAL ADVISORY
COMMITTEE FOR AERONAUTICS

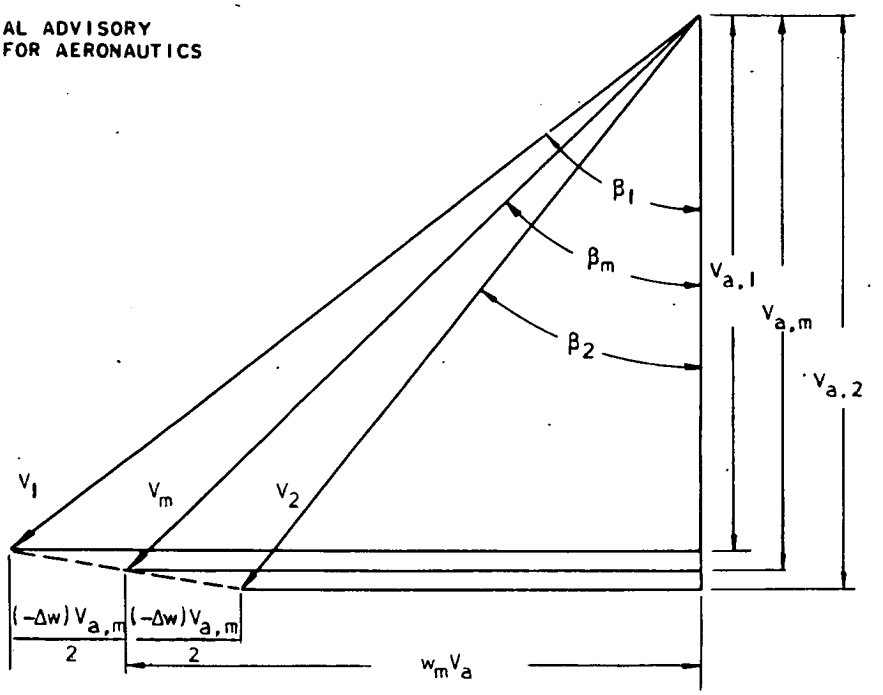

(a) With variable axial velocity.

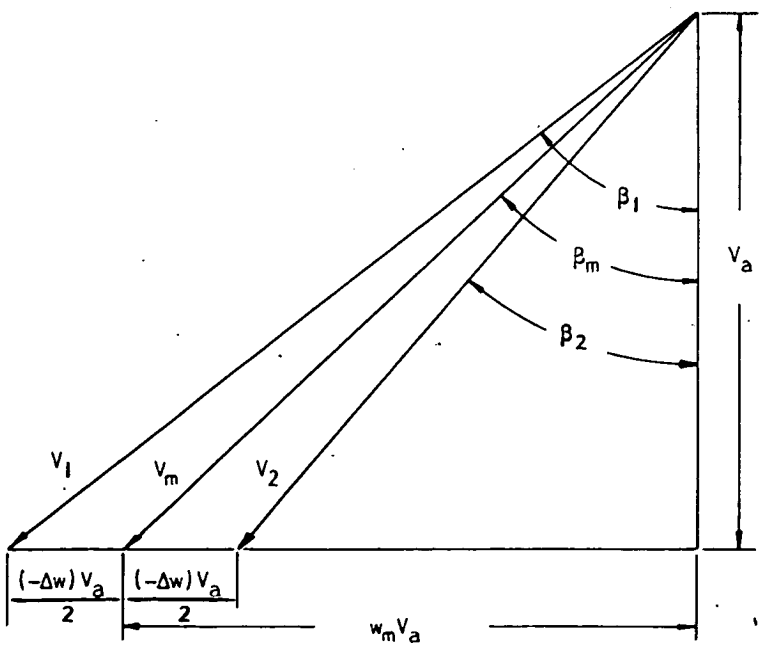

(b) With constant axial velocity.

Figure 1. - Relative-velocity diagram for typical blade row.

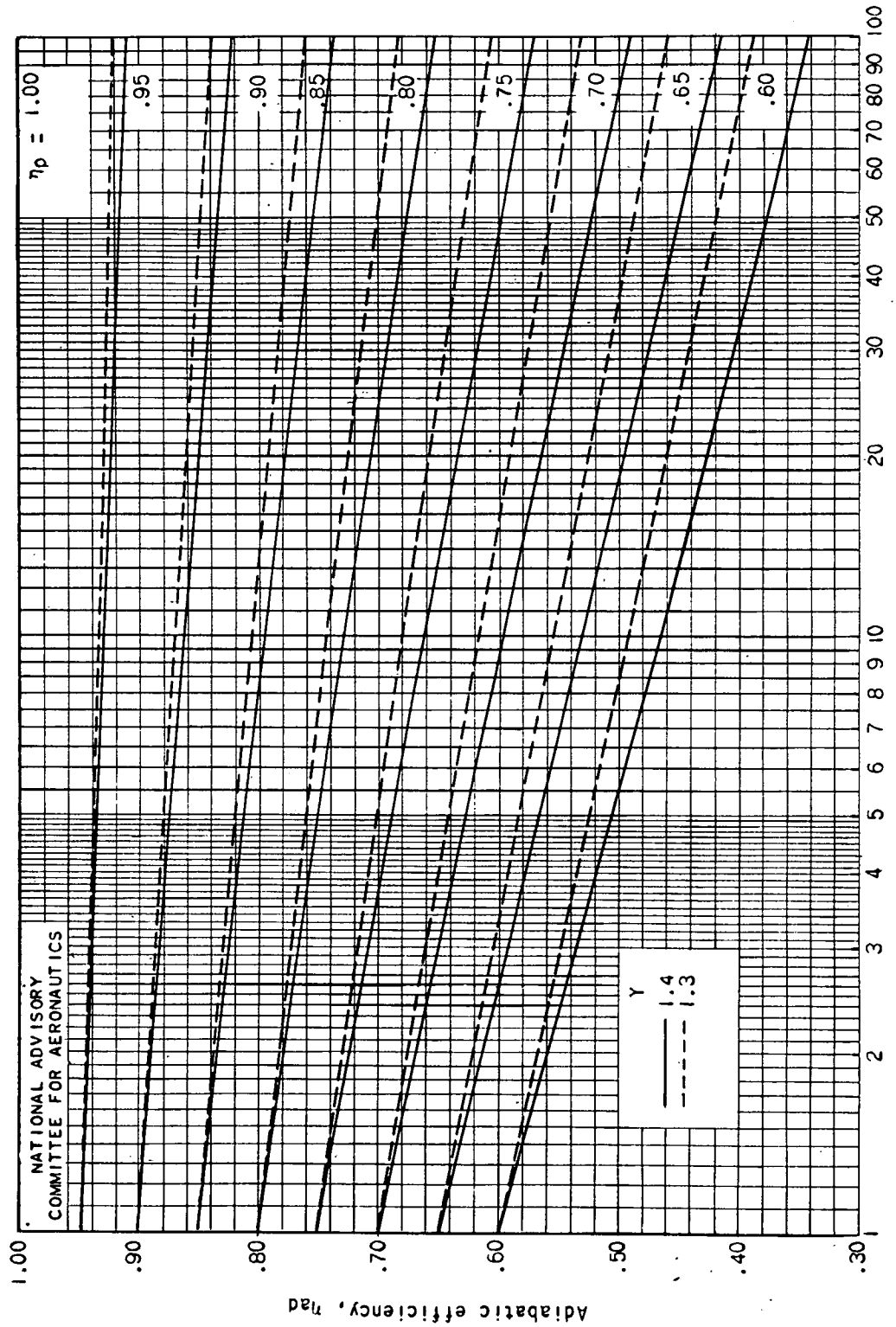

Figure 2. - Variation of adiabatic efficiency η_{ad} with pressure ratio for polytropic efficiencies η_p from 0.60 to 1.0 and γ equal to 1.3 and 1.4 for adiabatic compression.

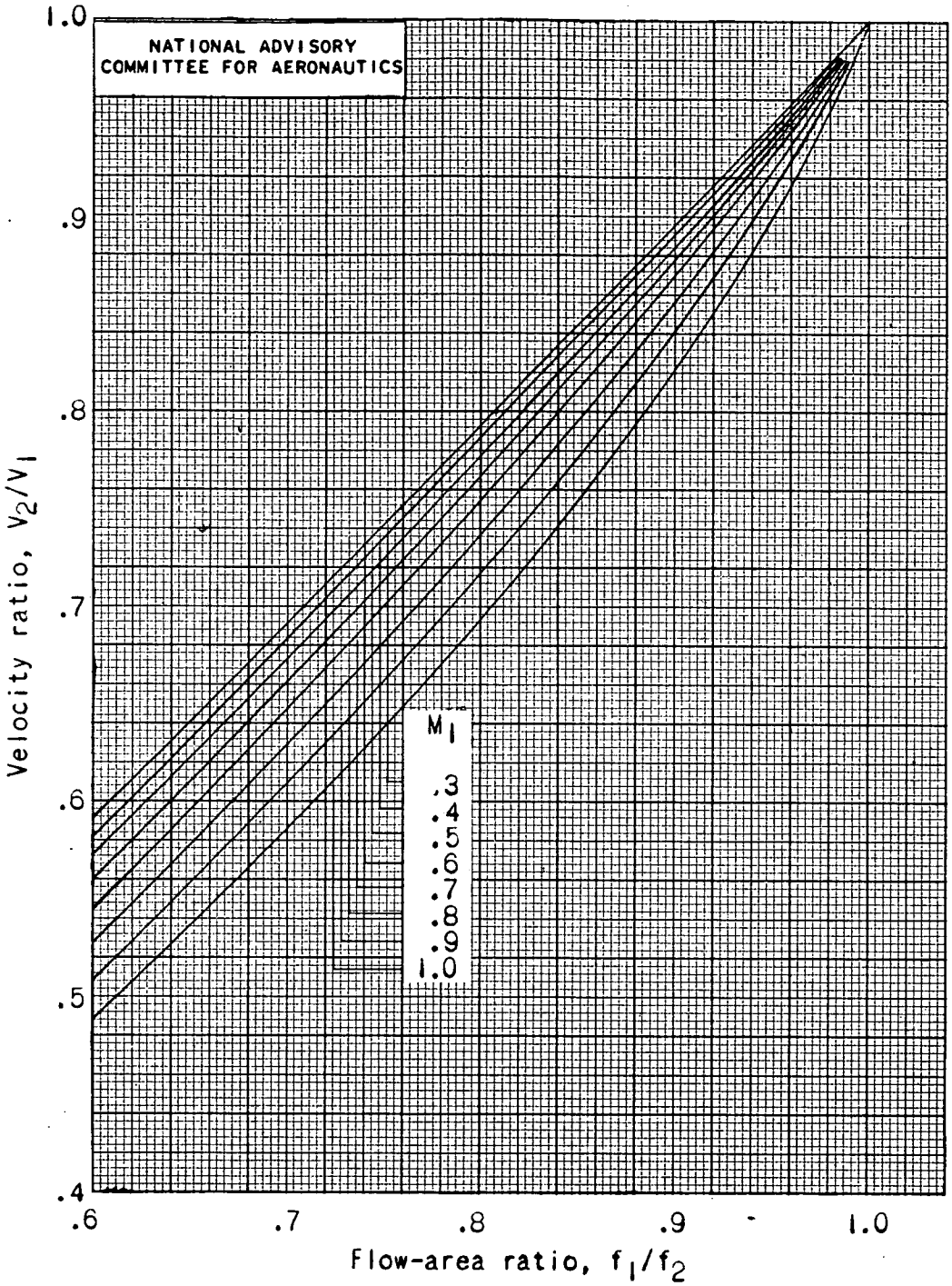

(a) Polytropic efficiency η_p, 0.7.

Figure 3. - Velocity ratio for steady, one-dimensional flow as a function of flow-area ratio, inlet Mach number, and polytropic efficiency for adiabatic compression with γ equal to 1.4.

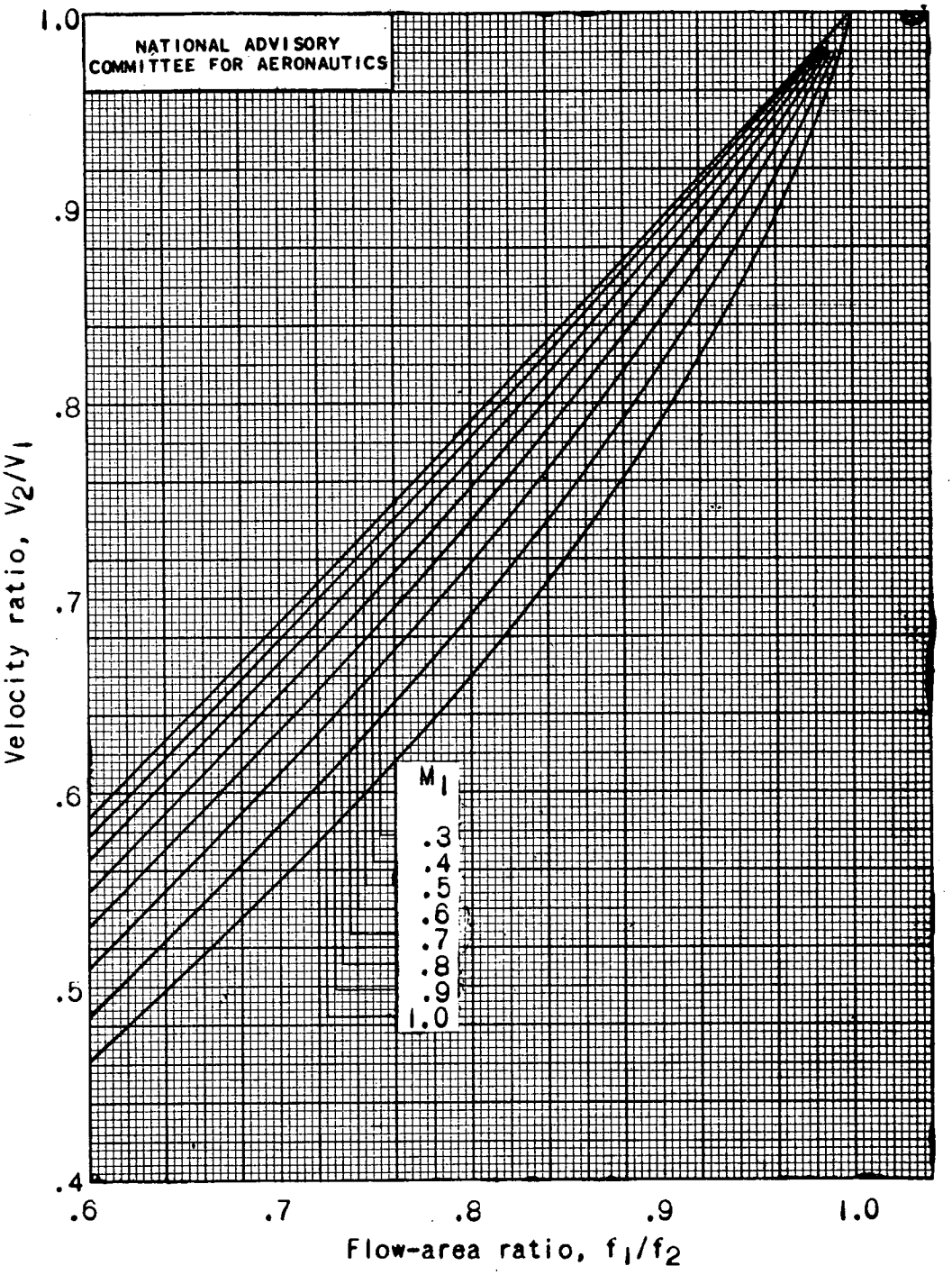

(b) Polytropic efficiency η_p, 0.8.

Figure 3. - Continued. Velocity ratio for steady, one-dimensional flow as a function of flow-area ratio, inlet Mach number, and polytropic efficiency for adiabatic compression with γ equal to 1.4.

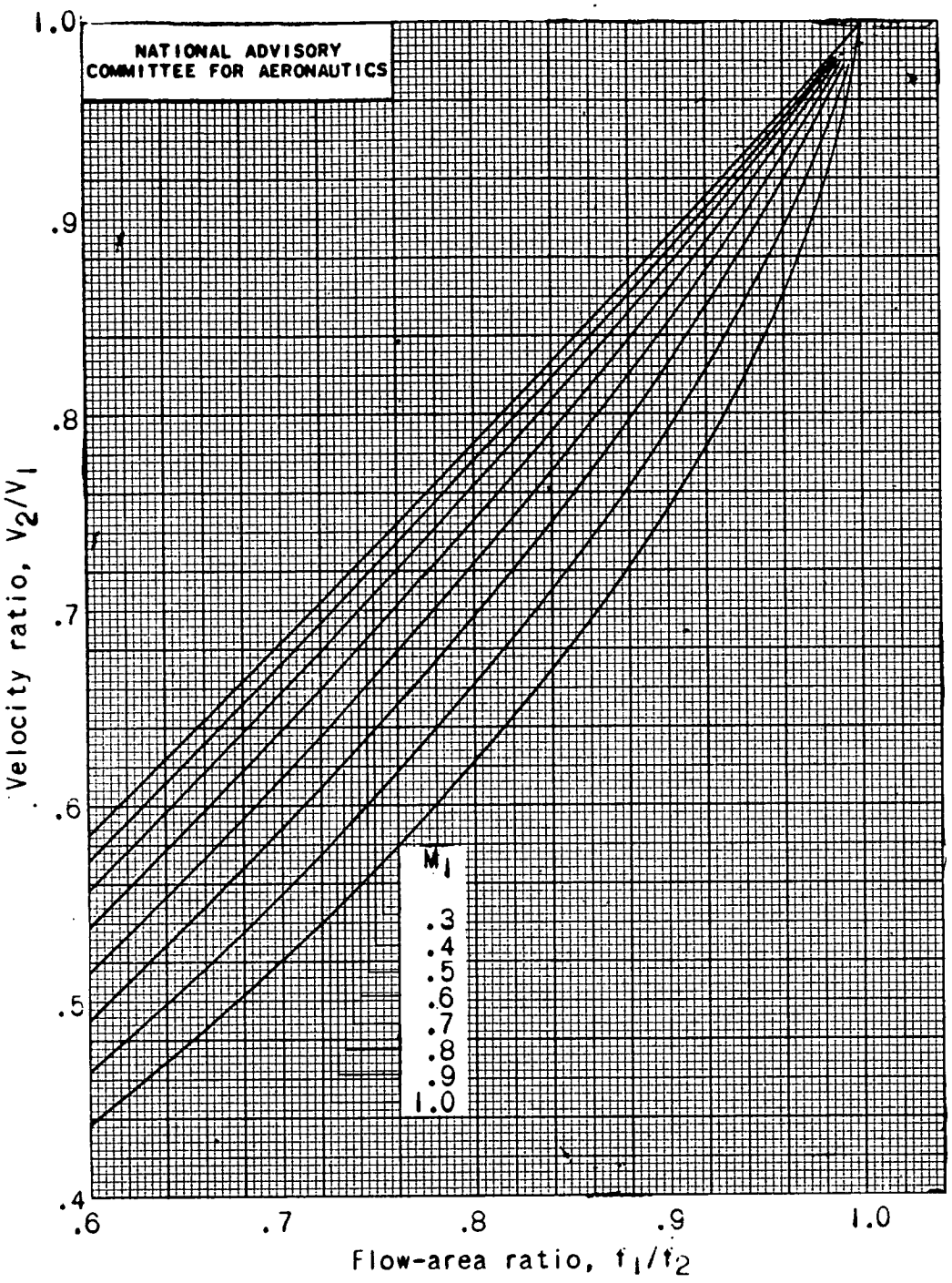

(c) Polytropic efficiency η_p, 0.9.

Figure 3. - Continued. Velocity ratio for steady, one-dimensional flow as a function of flow-area ratio, inlet Mach number, and polytropic efficiency for adiabatic compression with γ equal to 1.4.

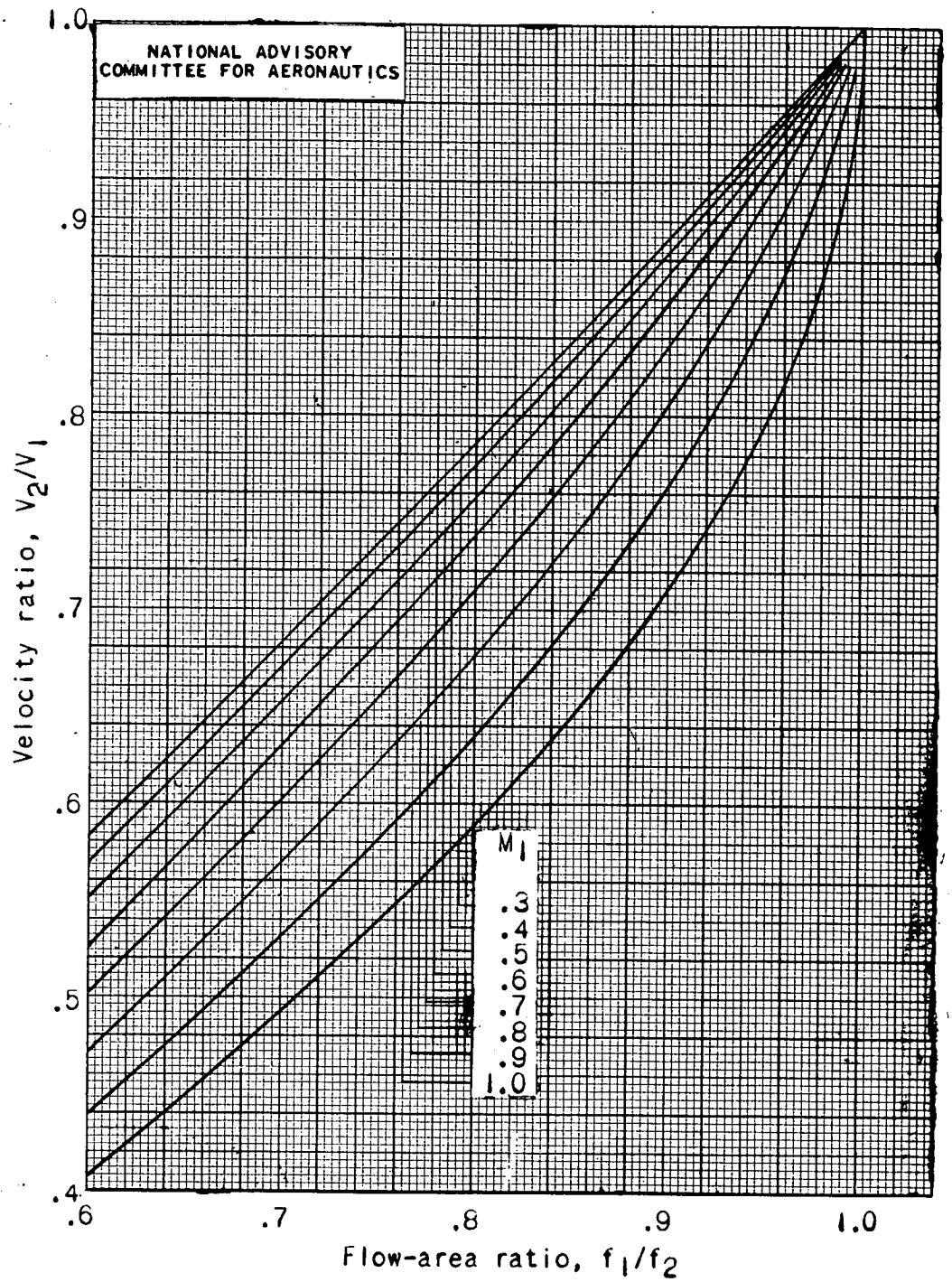

(d) Polytropic efficiency η_p, 1.0.

Figure 3. - Concluded. Velocity ratio for steady, one-dimensional flow as a function of flow-area ratio, inlet Mach number, and polytropic efficiency for adiabatic compression with γ equal to 1.4.

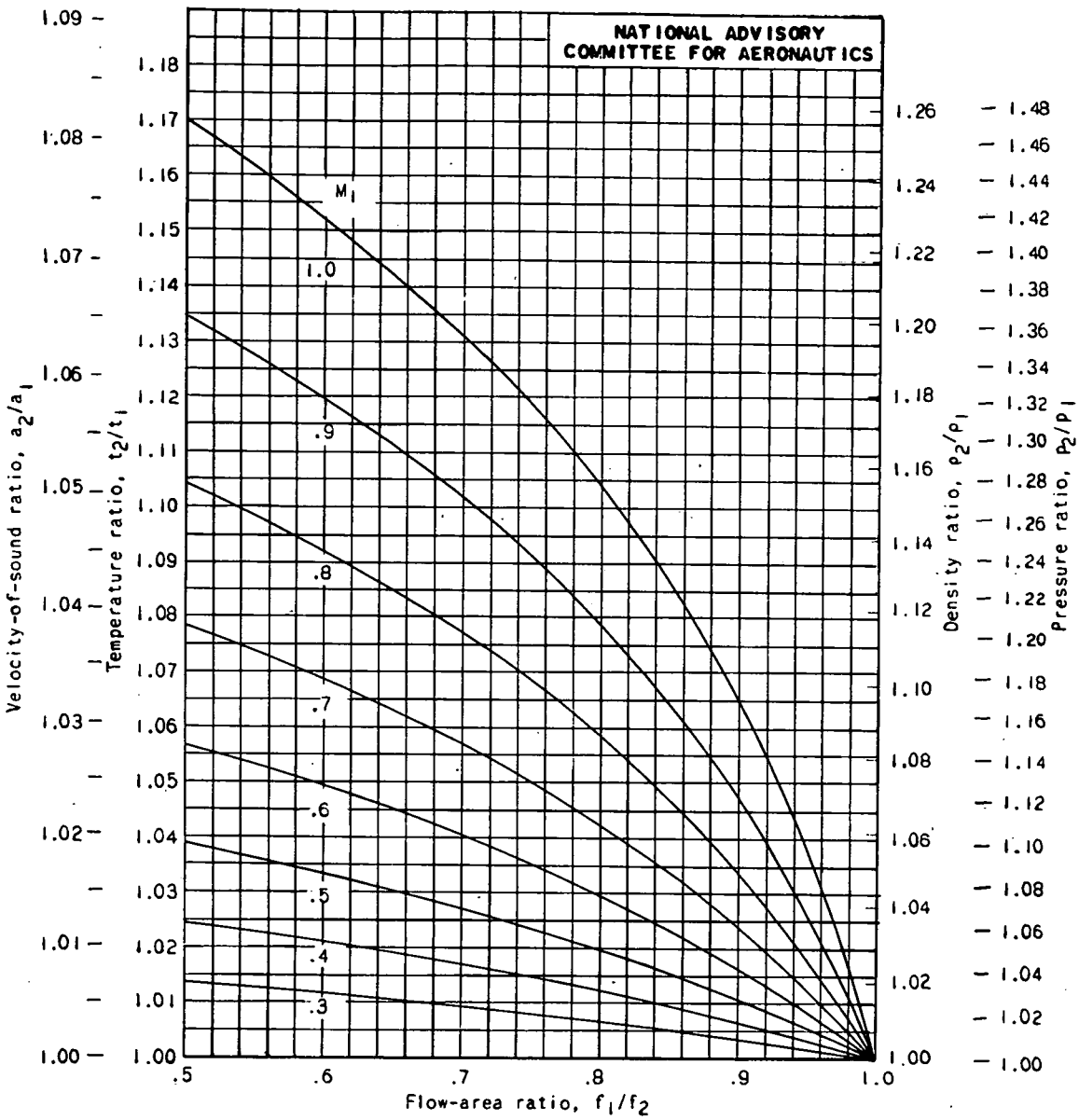

(a) Polytropic efficiency η_p, 0.7.

Figure 4. - Velocity-of-sound ratio, temperature ratio, density ratio, and pressure ratio for steady, one-dimensional flow as functions of flow-area ratio, inlet Mach number, and polytropic efficiency for adiabatic compression with γ equal to 1.4.

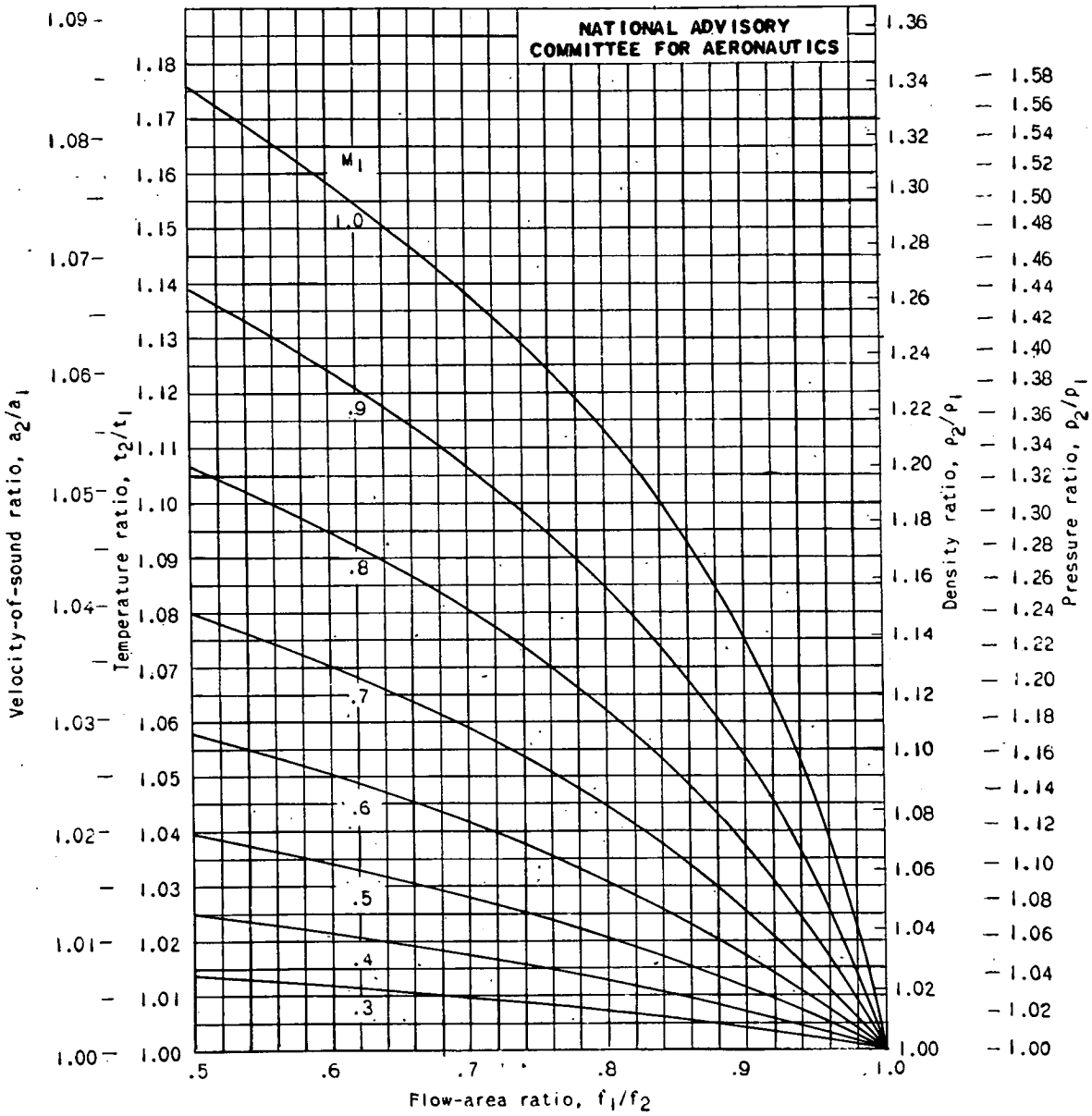

(b) Polytropic efficiency η_p, 0.8.

Figure 4. - Continued. Velocity-of-sound ratio, temperature ratio, density ratio, and pressure ratio for steady, one-dimensional flow as functions of flow-area ratio, inlet Mach number, and polytropic efficiency for adiabatic compression with γ equal to 1.4.

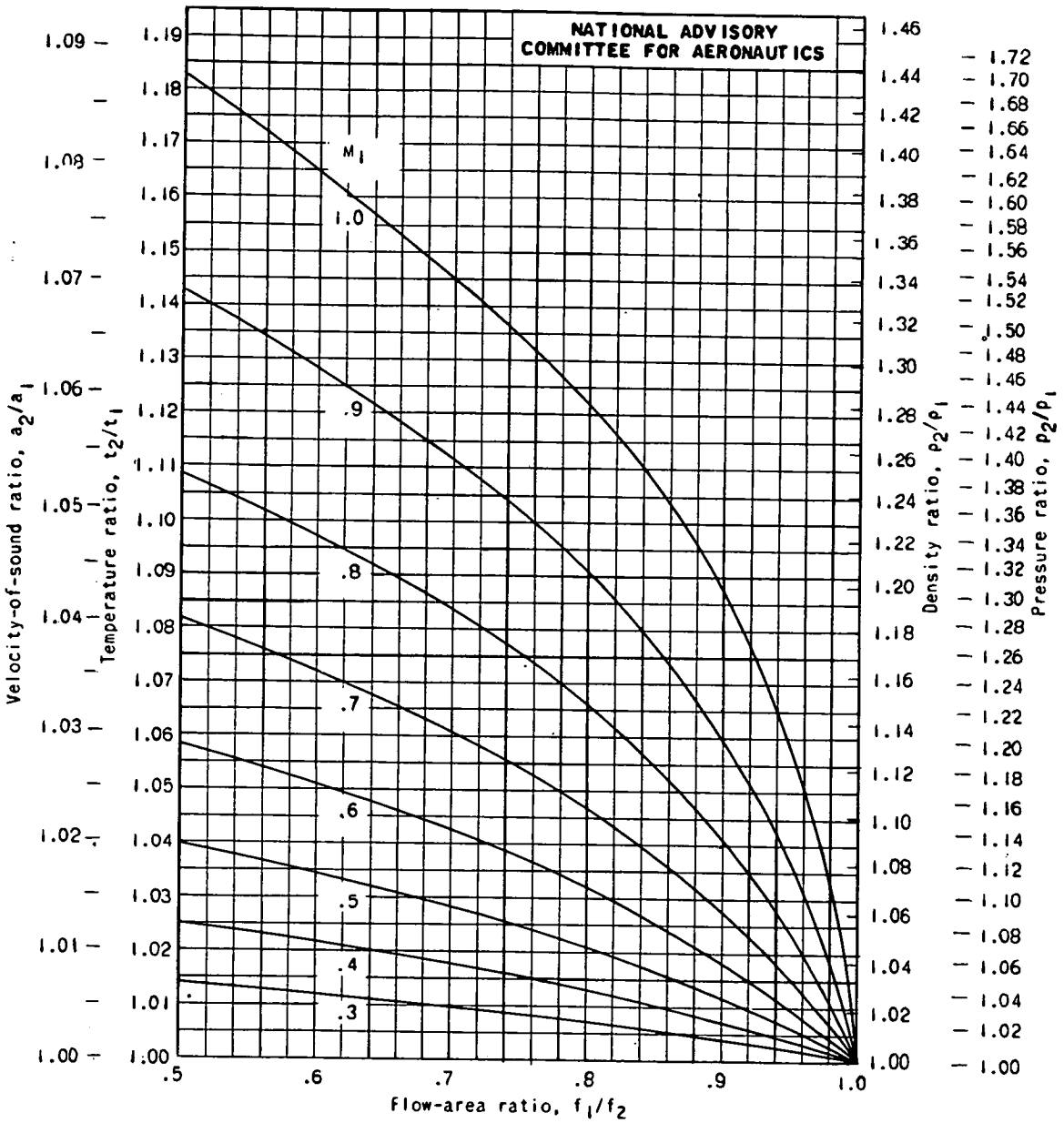

(c) Polytropic efficiency, η_p, 0.9.

Figure 4. - Continued. Velocity-of-sound ratio, temperature ratio, density ratio, and pressure ratio for steady, one-dimensional flow as functions of flow-area ratio, inlet Mach number, and polytropic efficiency for adiabatic compression with γ equal to 1.4.

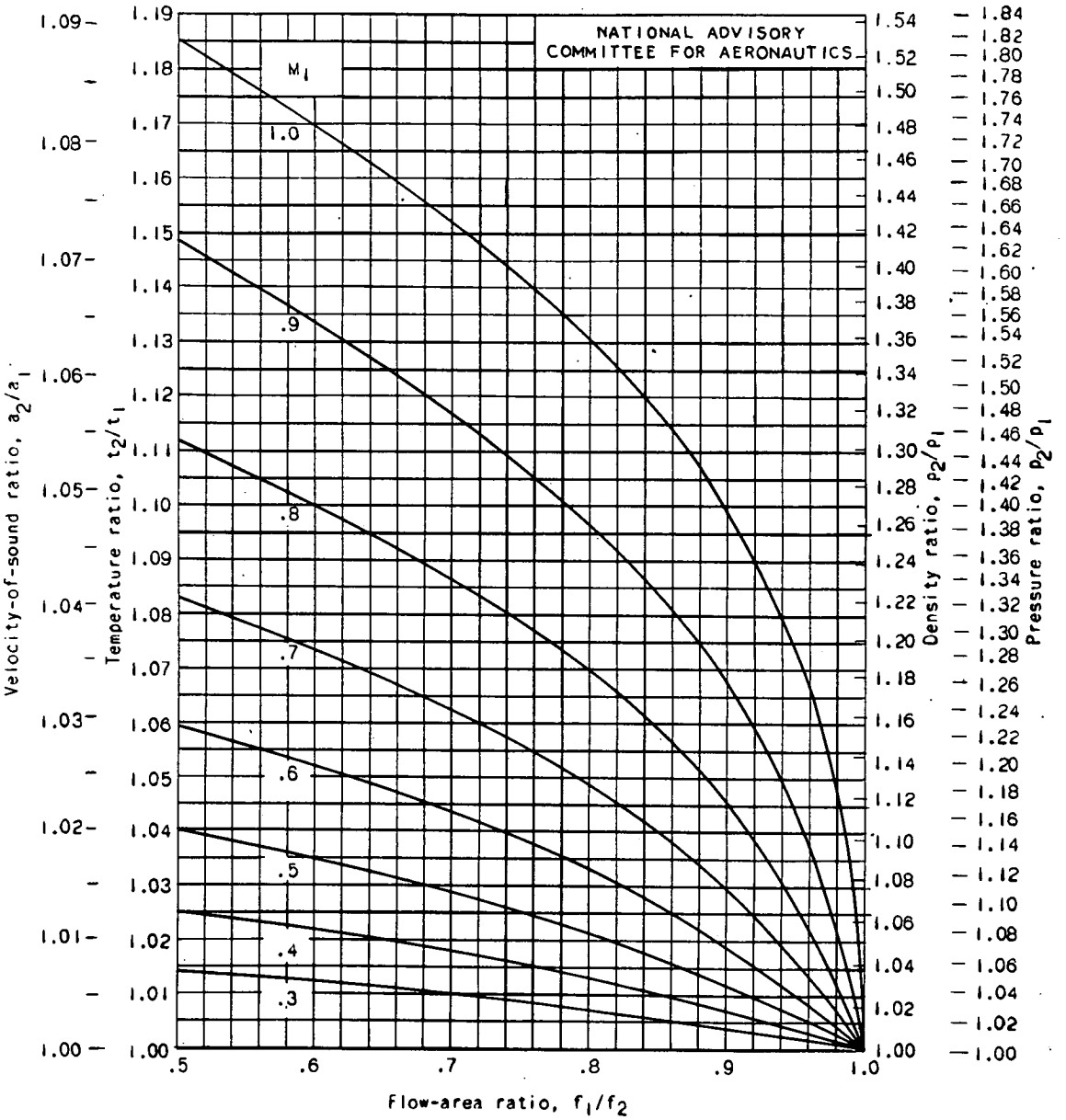

(d) Polytropic efficiency, η_p, 1.0.

Figure 4. - Concluded. Velocity-of-sound ratio, temperature ratio, density ratio, and pressure ratio for steady, one-dimensional flow as functions of flow-area ratio, inlet Mach number, and polytropic efficiency for adiabatic compression with γ equal to 1.4.

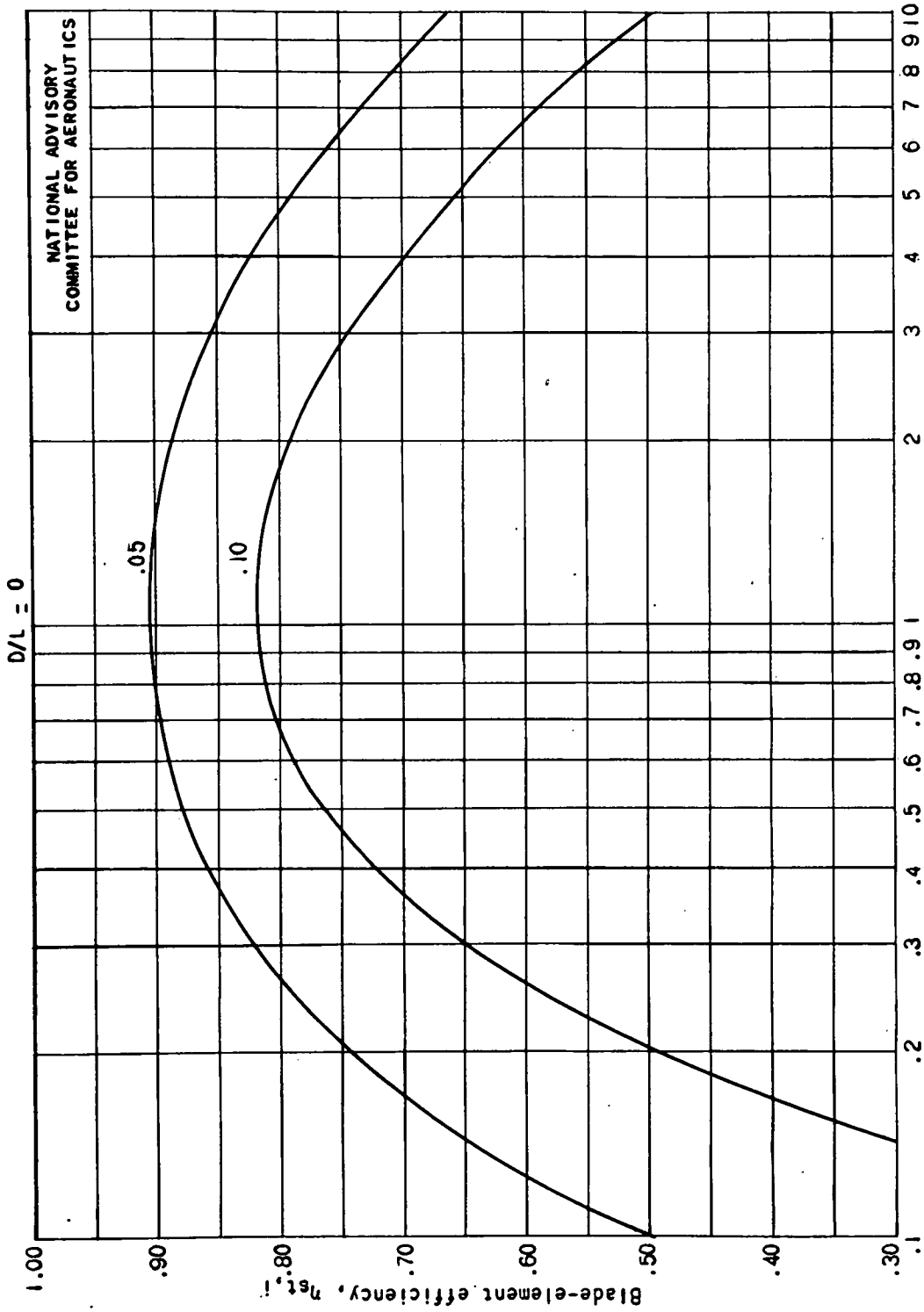

Figure 5. - Efficiency of blade element as function of w_m for D/L equal to 0, 0.05, and 0.10.

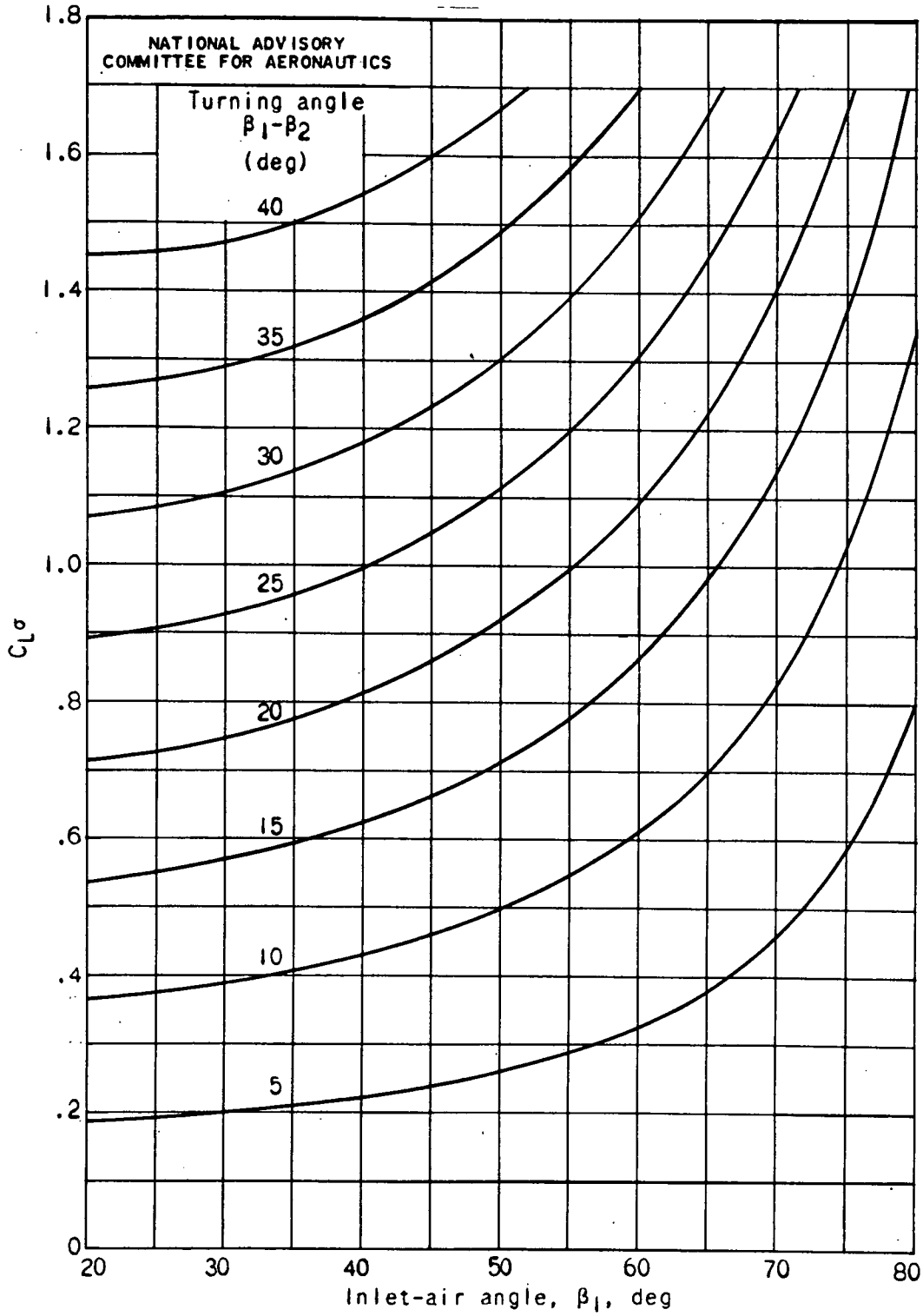

Figure 6. - Relation between $C_L\sigma$, inlet-air angle, and turning angle for D/L equal to 0.

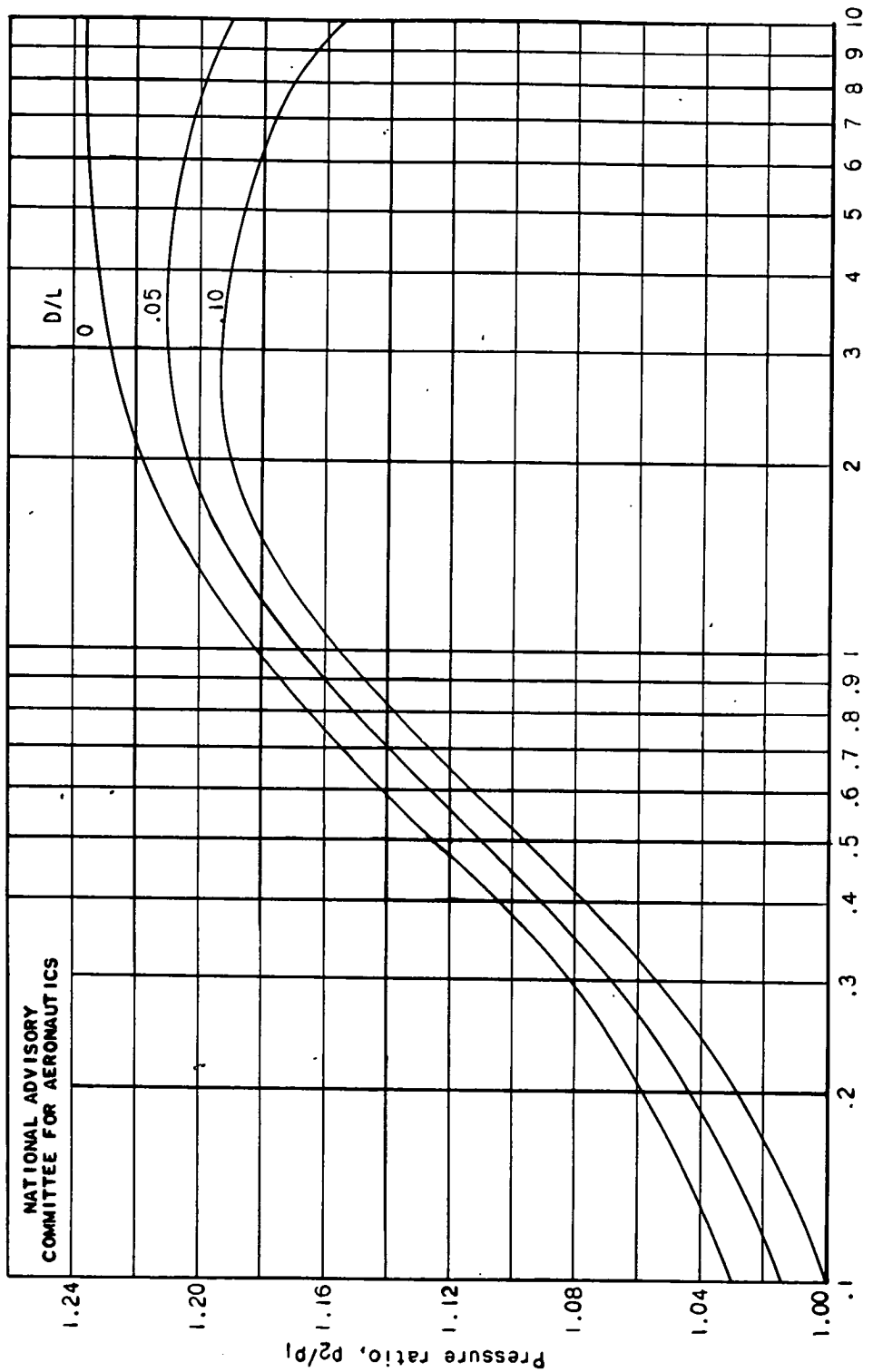

(a) M_1, 0.7; $C_{L\sigma}$, 1.0;

Figure 7. - Pressure ratio across blade row as a function of w_m.

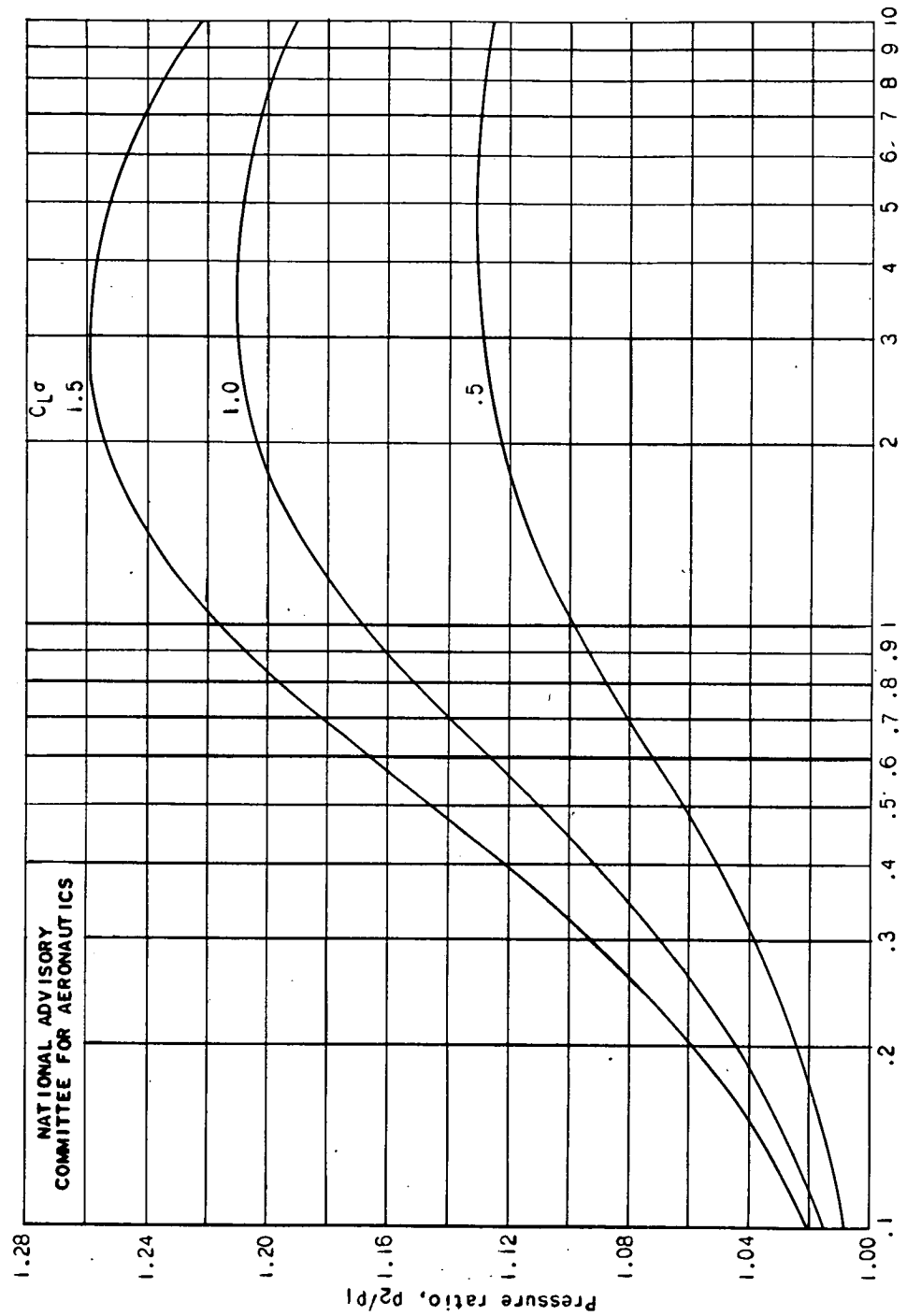

(b) M_1, 0.7; D/L, 0.05.

Figure 7. - Continued. Pressure ratio across blade row as a function of w_m.

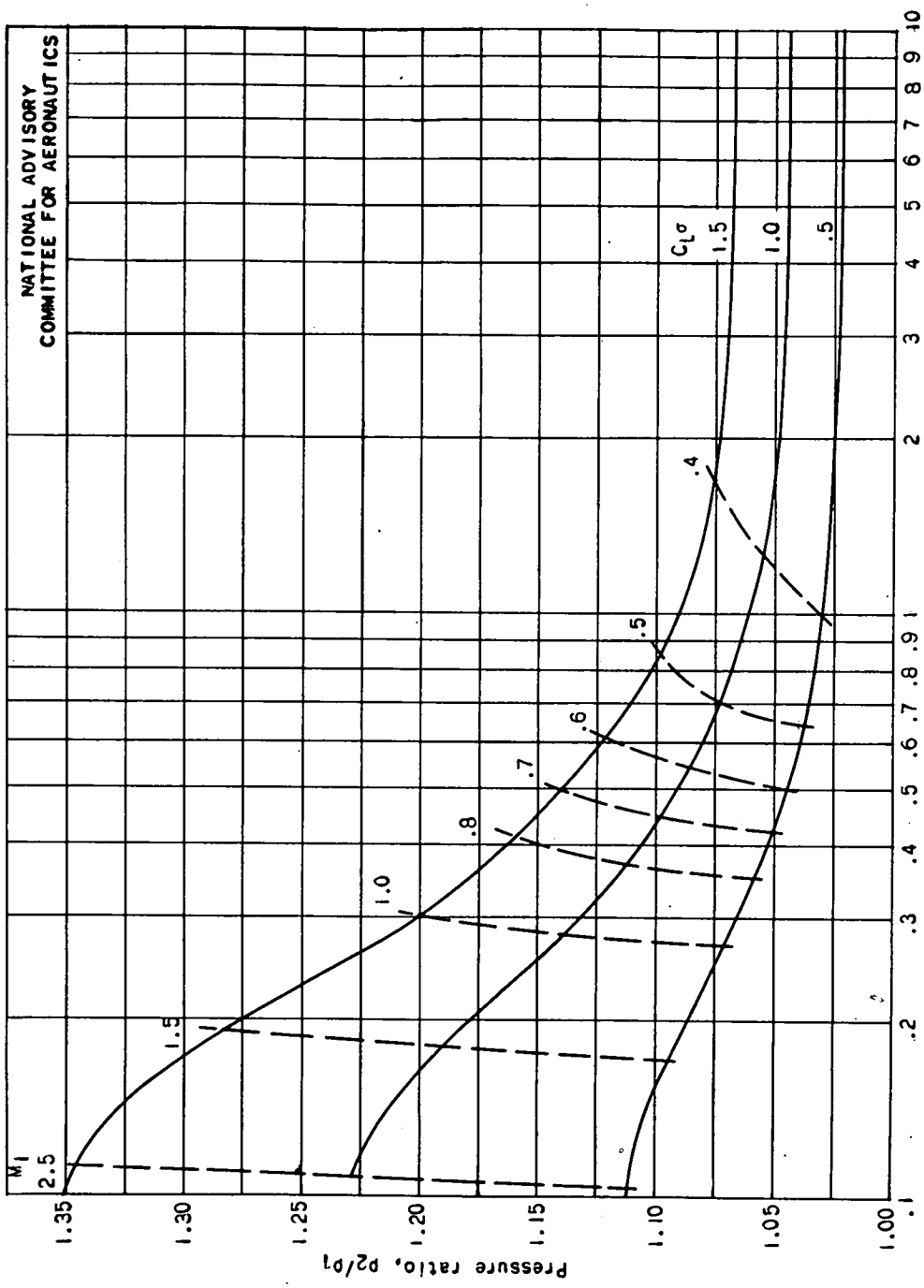

(c) U/a_1, 0.5; D/L, 0.05; symmetrical velocity diagram.

Figure 7. - Continued. Pressure ratio across blade row as a function of w_m.

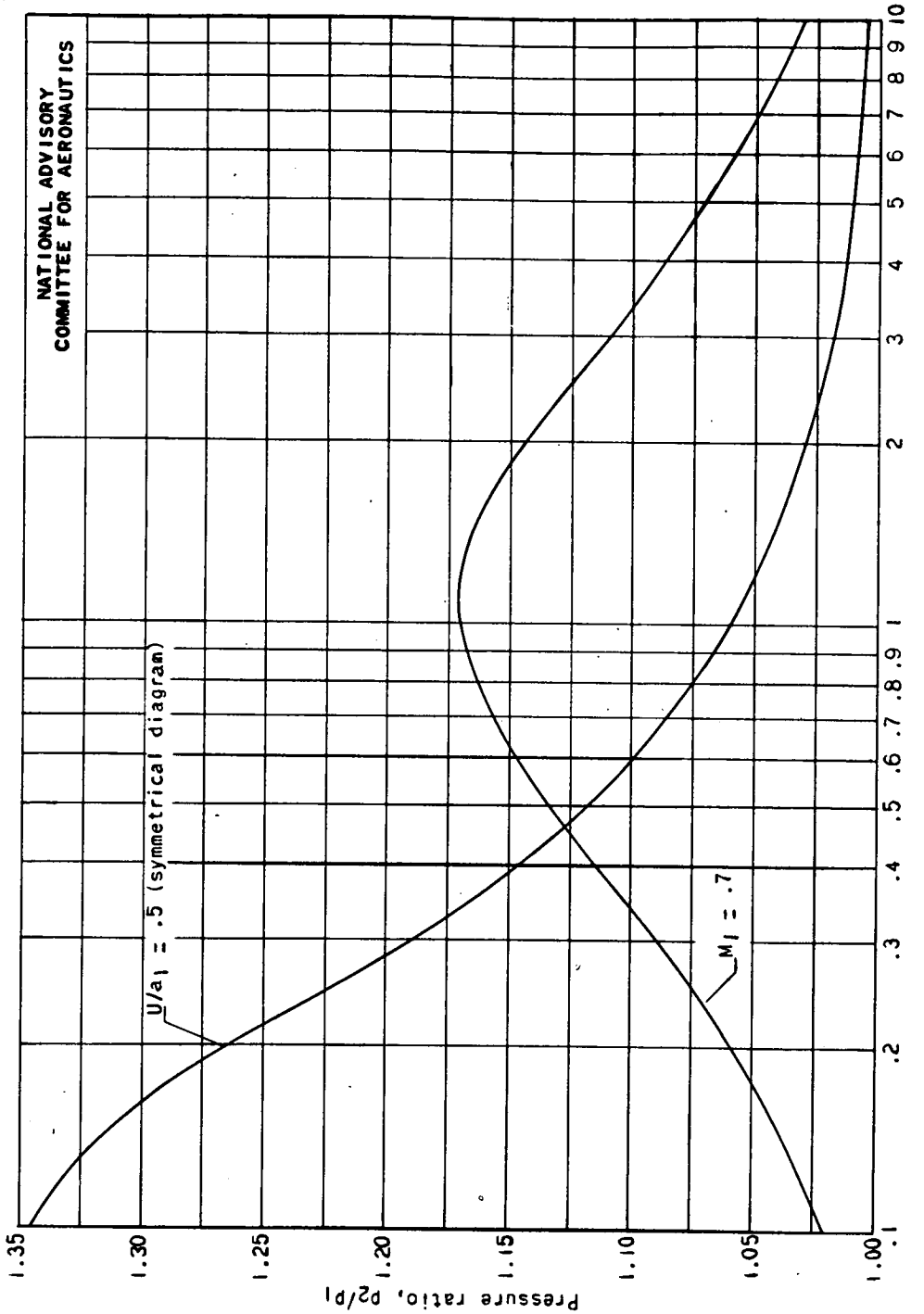

(d) $-\Delta w$, 0.7424; D/L, 0.05.

Figure 7. - Concluded. Pressure ratio across blade row as a function of w_m.

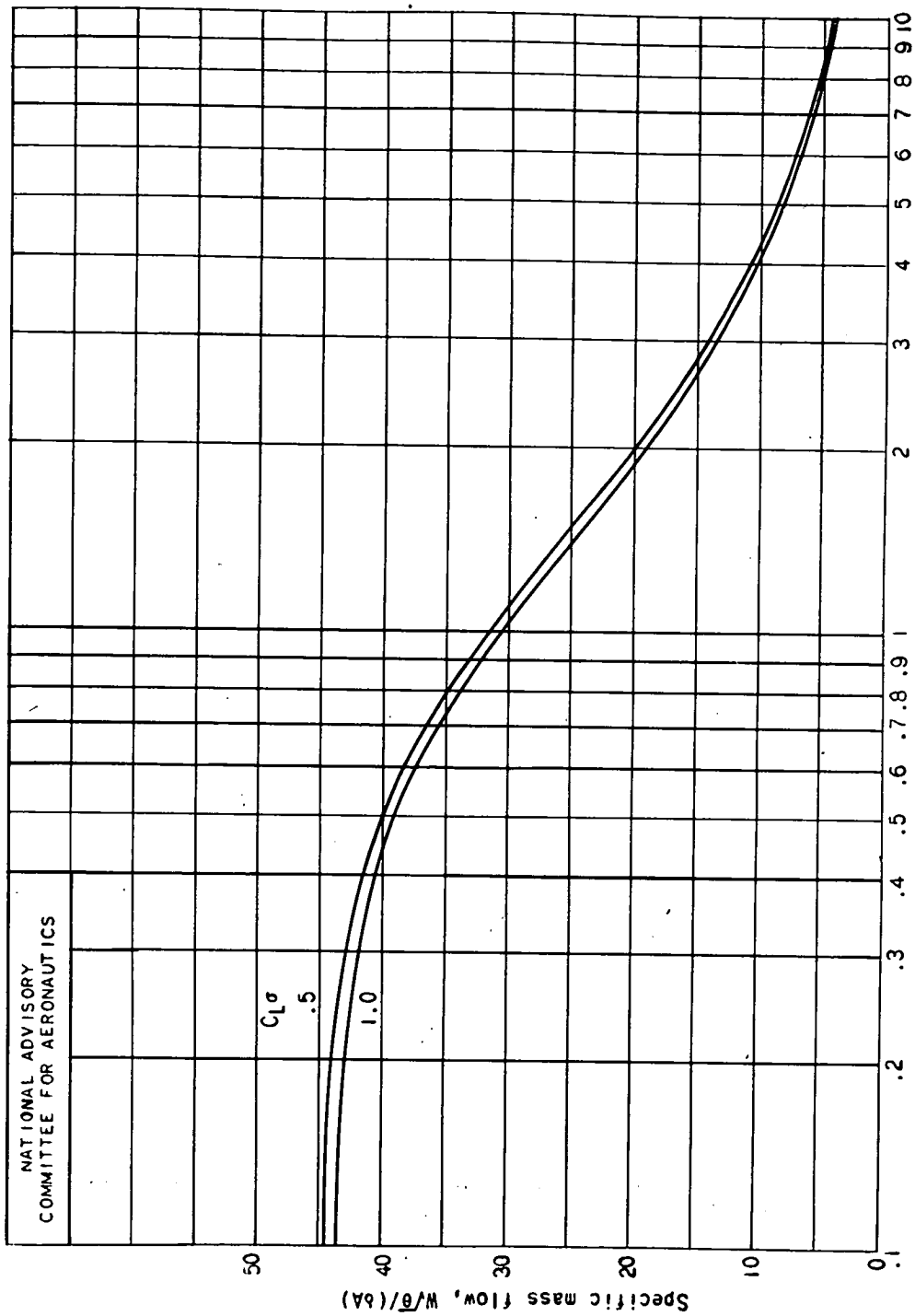

Figure 8. - Specific mass flow as a function of w_m for M_1 equal to 0.7, $C_{L\sigma}$ equal to 0.5 and 1.0 and a symmetrical velocity diagram.

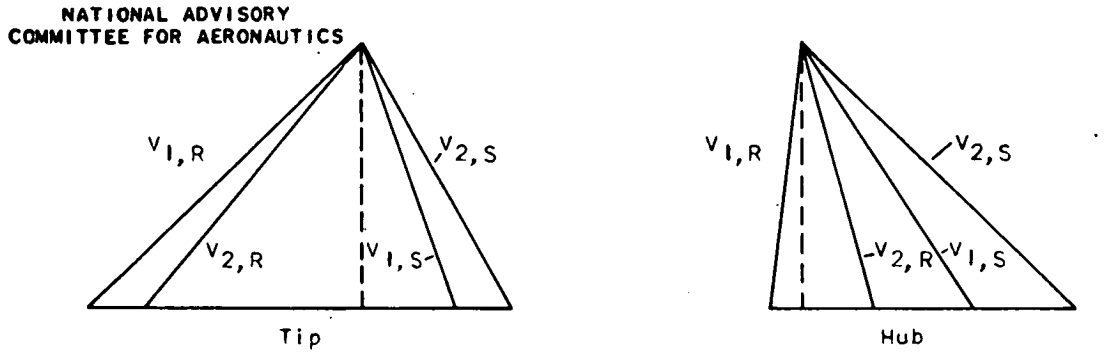

(a) Based on free vortex.

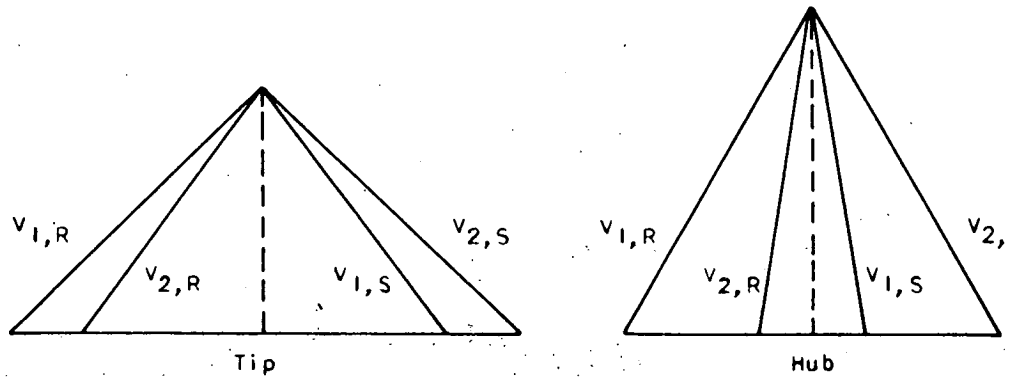

(b) Based on symmetrical velocity diagram and constant total enthalpy along radius.

Figure 9. – Velocity diagrams for entrance stage of multistage compressor for high specific mass flow with hub-tip diameter ratio of 0.55 and $(C_L\sigma)_{max}$ equal to 0.77.

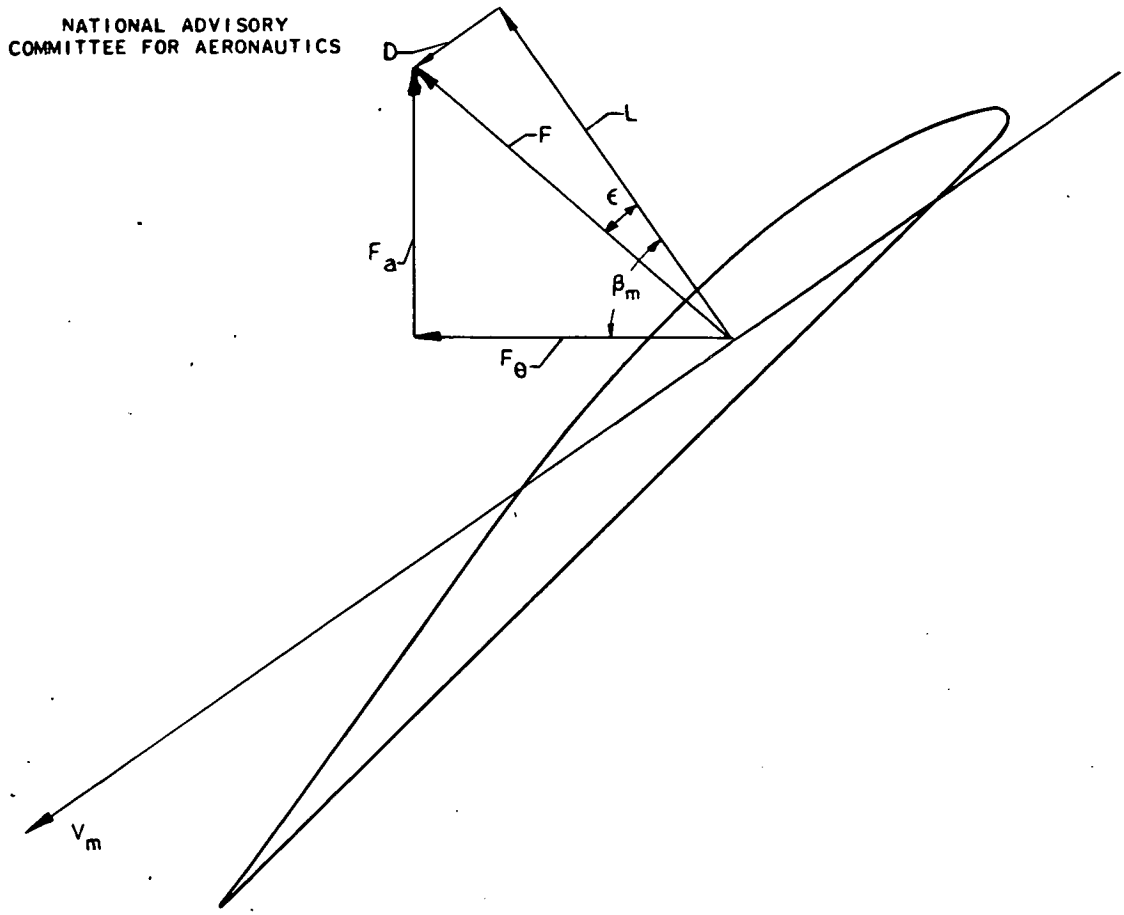

Figure 10. - Forces on blade element.